

REPORT

N° 34/2016

**EVALUATION OF A VACCINE (INFANRIX) SAMPLE THROUGH AN
ENVIRONMENTAL SCANNING ELECTRON MICROSCOPY
INVESTIGATION AND AN X-RAY MICRO-ANALYSIS**

Client : UNACS

Sample checked : Vaccine Infanrix

Analyses and conclusions by: Dr. Antonietta Gatti, Dr. Stefano Montanari

Signatures:

Date: San Vito, 22nd August 2016

This report is made up of 41 (forty-one) numbered pages including the cover.

Note:

The results may be referred only to the material checked and the type of application requested.

In case this report should be reproduced, the Client or any other person or agency in its possession engage themselves to do that only in full form.

Any partial reproduction must be authorized in written form by Nanodiagnostics srl.

INDEX

1. INTRODUCTION	3
2. MATERIAL	4
3. TEST CONDITIONS.....	5
4. TIPES OF ANALYSES CARRIED OUT	6
5. RESULTS.....	6
INFANRIX – vaccine distributed in France (Lot A21CC421A – expiry date 04/2017)	7
6. DISCUSSION AND CONCLUSIONS	36
7. REFERENCES.....	37

1. INTRODUCTION

Nanodiagnostics srl is a consulting firm in the fields of medicine, biology, industry, environment and ecology. Its main activity is detecting inorganic micro- and nano-particles in any medium (biological tissues, food, drugs, cosmetics, environmental samples, garments, etc.), through an innovative system of environmental scanning electron microscopy. The investigation is carried out mainly by means of an ESEM or a FEG - ESEM (Field Emission Gun - Environmental Scanning Electron Microscope, QUANTA 200, FEI Company, Holland) with suitable protocols according to the type of substrate.

This analysis offers the possibility to observe biological samples in wet-mode, i.e. in the condition of their normal hydration, at environmental pressure, without the need to dehydrate them or make them electro-conductive through a coating of Carbon, or metals like Gold and Palladium, a procedure that is necessary with the traditional scanning electron microscopes.

By applying appropriate protocols to be adapted to each kind of observation, this feature allows to check biological samples, including living cells, without impairing their integrity, and to repeat the test every time one wishes. The main objective of the study is the detection of inorganic micro- and nano-particulate matter, in case there should be any in the sample, and this is achieved without the need of any process of the specimen.

An x-ray microprobe of an EDS (Energy Dispersive System, EDAX, USA) supplements the investigation, as the spectrum thus obtained shows the chemical elemental composition of the particulate matter. In fact, it measures the energy characteristic of each element making up the particles in the specimen, and returned as X-rays after the sample has been hit by the electron beam delivered by the FEG - ESEM.

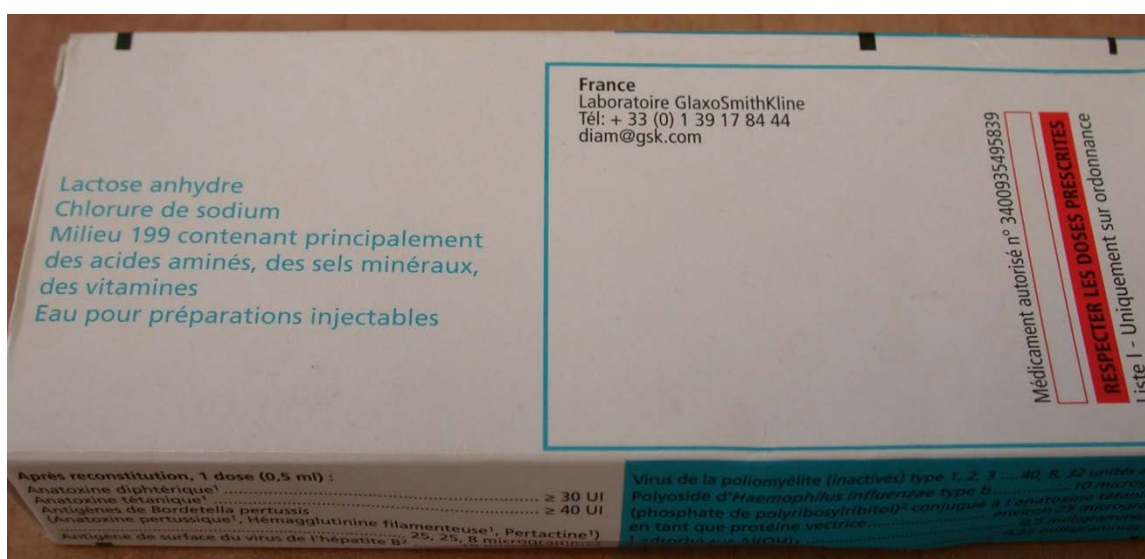
So, through such an integrated analysis, the micro- and nano-sized inorganic particles are photographed, measured and chemically characterized in a non-invasive, non-destructive, repeatable way, the only exception being fluids, which are often hard to recover in their liquid form after some time. (1,2,3)

The investigation can be carried out on specimens of biological origin like biopsies, autopsies and organic fluids, but is equally feasible on many other kinds of materials like, for example, environmental samples, food, drugs or cosmetics. As the principal object of the investigation is inorganic and non biodegradable, there is no particular difficulty in detecting such particulate matter either in fresh or in archived samples.

2. MATERIAL

A whole package of vaccine INFANRIX by GlaxoSmithKline Biologicals s.a, distributed in France, was sent to the Laboratory (lot A21CC421A - expiry date 04/2017) for the ultrastructural analyses. The package contained a syringe pre-filled with injectable water, a vial containing the vaccine as powder and two sterile needles. The vaccine powder consists of 10 microg "Neisseria meningitidis" oligosaccharides. That was conjugated with 15 microg of CRM197 protein adsorbed on Aluminum phosphate (0.125 mg Al³⁺) in presence of saline.

The specimen was sent by UNACS and was encoder at the Laboratory as STD 1225.





3. TEST CONDITIONS

The sealed sample was preserved in a +4 °C refrigerator at the Laboratory until preparation. After verifying the integrity of the package, the package was opened inside a laminar-flow hood. The needle was connected to the syringe wearing talc-free gloves and the syringe was shook horizontally in order to make the solution homogeneous and simulate the procedure as suggested by the instructions for the use before administration.

Then, a drop of about 20 microliters of liquid was deposited on a nitrocellulose filter (Millipore, type HAWG, 0.45 micron) mounted on a Carbon disc, adherent to the Aluminum

stub for the electron-microscopy observation. Thus prepared, the sample was inserted in a specific, clean container, sealed and left to dry at room temperature inside the laminar-flow hood where the whole operations had been carried out.

After about 24 hours the sample was entered in the electron-microscope chamber for the analysis.

All procedures were carried out in an environment protected from environmental pollution and with clean instruments.

4. TIPES OF ANALYSES CARRIED OUT

The electron-microscopy study was meant to ascertain the presence of the declared inorganic components in the vaccine solution and to investigate on the presence of possible foreign bodies. The technique used was developed within the European project called Nanopathology (QLRT-2002-05-147) employing an environmental scanning electron microscope FEG – ESEM Quanta 200, by FEI (The Netherlands), that allows to observe solid micro- and nanoparticles in the sample investigated. The energy-dispersive X-ray spectroscopy carried out through an EDAX (USA) instrument allows to evaluate the elemental composition of the particles detected (1,2).

5. RESULTS

The electron-microscopy analyses of the sample showed the presence of particulate matter with different chemical compositions (see Table).

The chemical and morphological results are shown in the pictures that follow.

The spectrum peaks without an indication of the chemical element to which they refer are the secondary peaks of an already reported element at its primary peak.

Note: The list of the elements reported in the table is done according to their degree of representativeness, starting from the highest in the EDS spectrum.

INFANRIX – vaccine distributed in France (Lot A21CC421A – expiry date 04/2017)

The table contains all the most meaningful analyses carried out on the sample. The product contains Aluminum salts that create precipitates. Identification of further foreign bodies in the Al-precipitates was particularly hard.

N. analysis	Description (magnification, morphology)	Elements detected
1	Vaccine on filter – 60x	Morphology image
2	400x	
3	1486x	AlOClPNaCS
3BIS		OAlClPNaC
3TER		Subtraction 3-3bis=AlCl
4	19594x (54 spherules 0.5m)	OWAlPNaClCaCSFe
5		38236x
6	Debris 5 µm, 6971x	OAlWPCINaCaSFe
7	10582x	OAlWPCINaCaSFe
8	6 µm; 10103x	WAICa
9	2-1-0.5 µm, 40000x	OWAlCaClNaPCFe
10	5287x	
11	2007x	AlOClNaP/OAlPCINa
		Subtraction 11-11bis, AlClOClNaP
12	2252x	
13	dx5 µm + 0.8 µm 6988x	FeOAlCrNiClPNaSiMn/ OWAlCaClNaPCFe
14	3808x	OWAlCaClNaPCFe
15	1.5 µm, 4998x	OWAlCaClNaPCFe
16	5 µm, 10235x	TiAlOPNaCl
17	8807x	OWAlCaClNaPCFe
18	4597x	OWAlCaClNaPCFe
19	5185x	OWAlCaClNaPCFe
20	2986x	OWAlCaClNaPCFe
21	White block 50 µm, 5185x	OAlPCINaC + OWAlCaClNaPCFe
22	22484x	OWAlCaClNaPCFe
23	protein corona, 40000x	OWAlCaClNaPCFe
24	13490x	OWAlCaClNaPCFe
25	spherules W, 32180x	OWAlCaClNaPCFe
26	cubes W, 64479x	OWAlCaClNaPCFe
27	62x	OWAlCaClNaPCFe
N. analysis	Description(magnification,	Elements detected

	morphology)	
28	1599x	OWAIaClNaPCFe
29	2895x	OWAIaClNaPCFe
30	12477x	OWAIaClNaPCFe
31	2404x	W

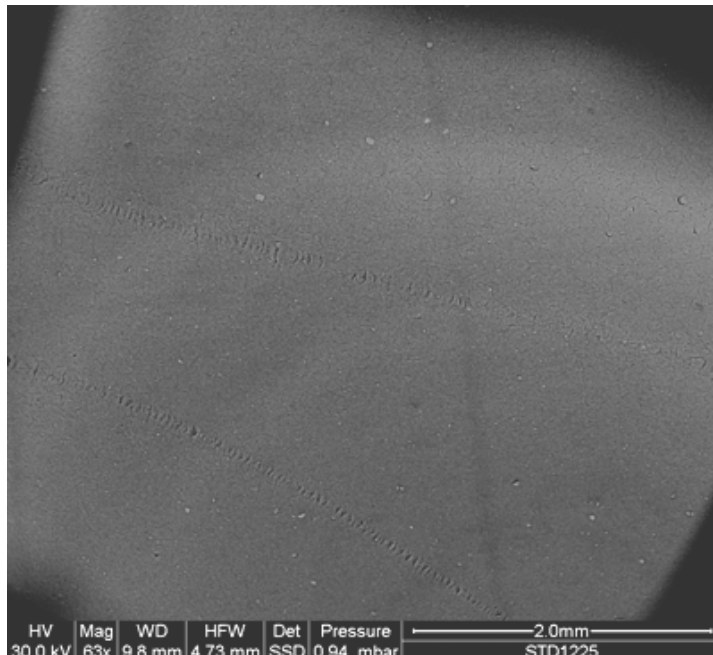


Image 1. The low-magnification (60x) image shows the surface of the nitrocellulose filter on which the droplet of vaccine was deposited.

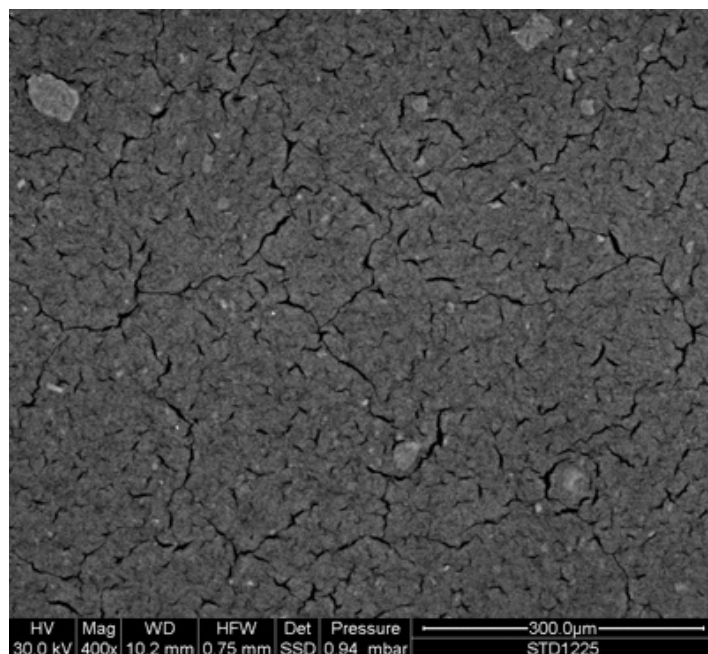


Image 2. The medium-magnification (400x) picture shows a section of the sample where crystals and precipitates are visible.

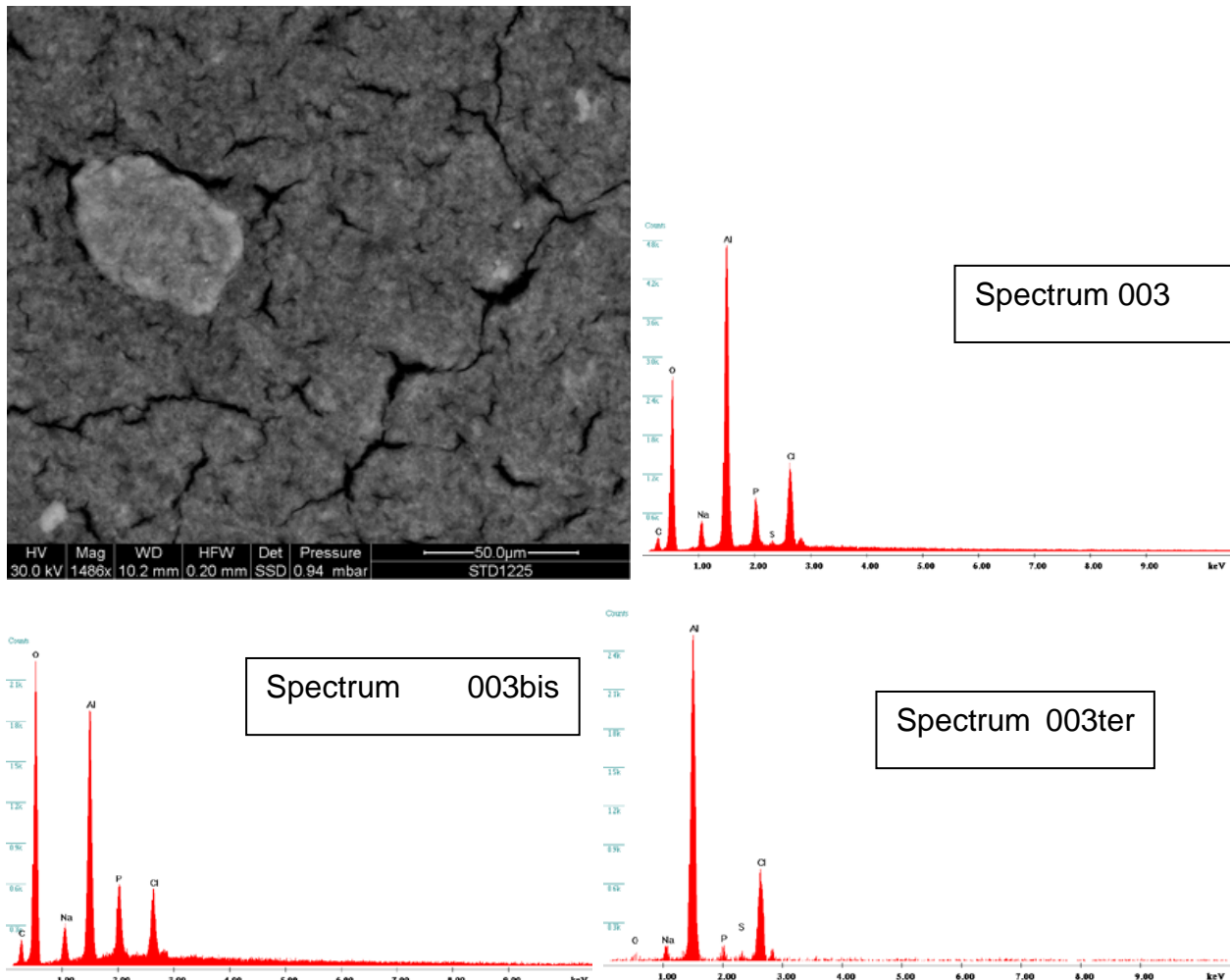


Image 3. A section of the sample is shown at high magnification (1486x). A 50-micron detritus is visible. The EDS analysis shows its composition: Aluminum, Oxygen, Chlorine, Sodium, Carbon, Sulfur. The filter is completely covered by Aluminum-phosphate salts including Sodium chloride.

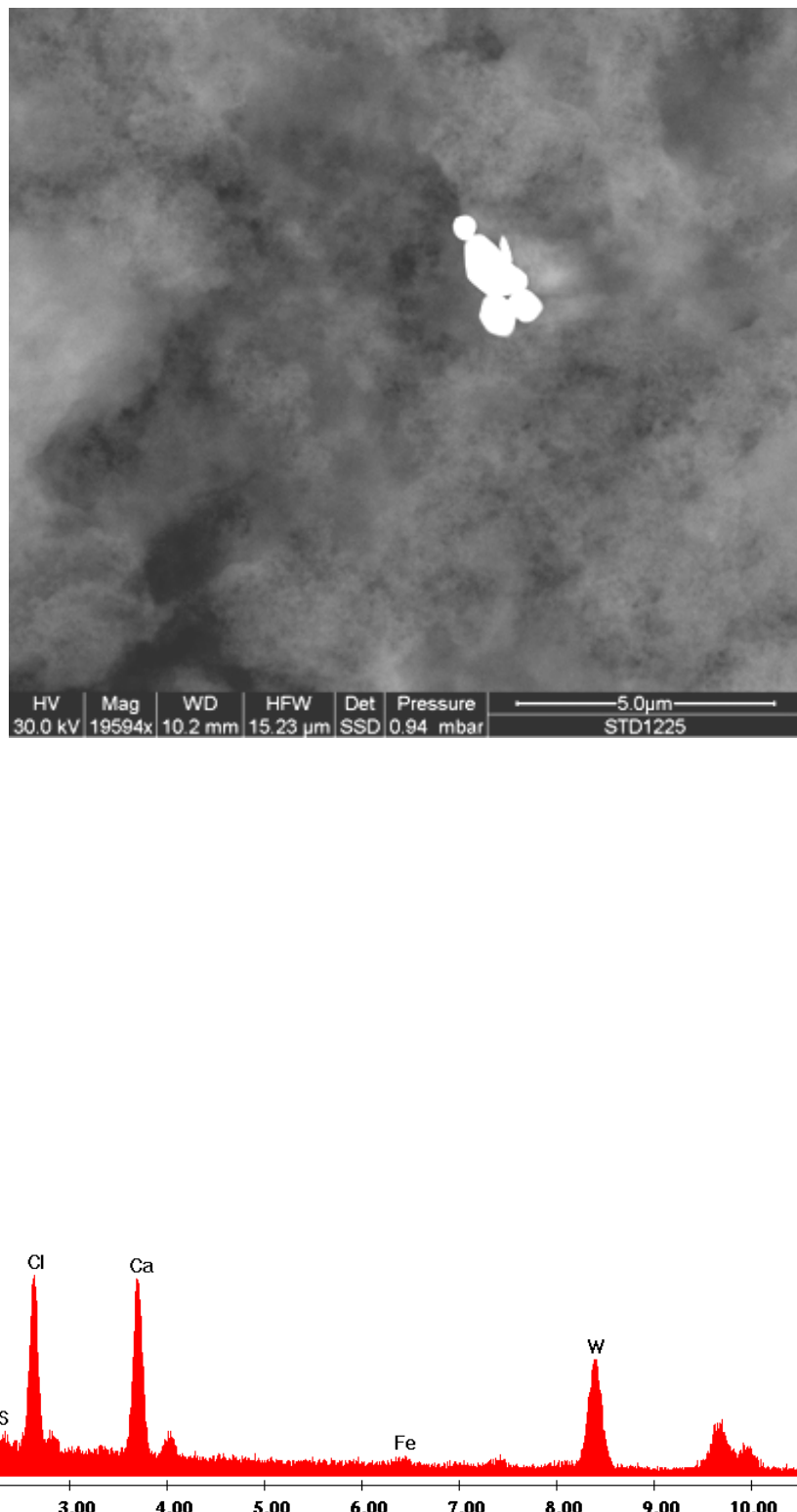


Image 4. A high-magnification (19594x) section of the sample is shown where clustered particles of Oxygen, Tungsten, Aluminum, Phosphorous, Sodium, Chlorine, Calcium, Carbon, Sulfur and Iron are visible. The size of the cluster is about 3 microns. This is a foreign body composed of Tungsten-Calcium-Iron not belonging to the vaccine's, or to any drugs', composition.

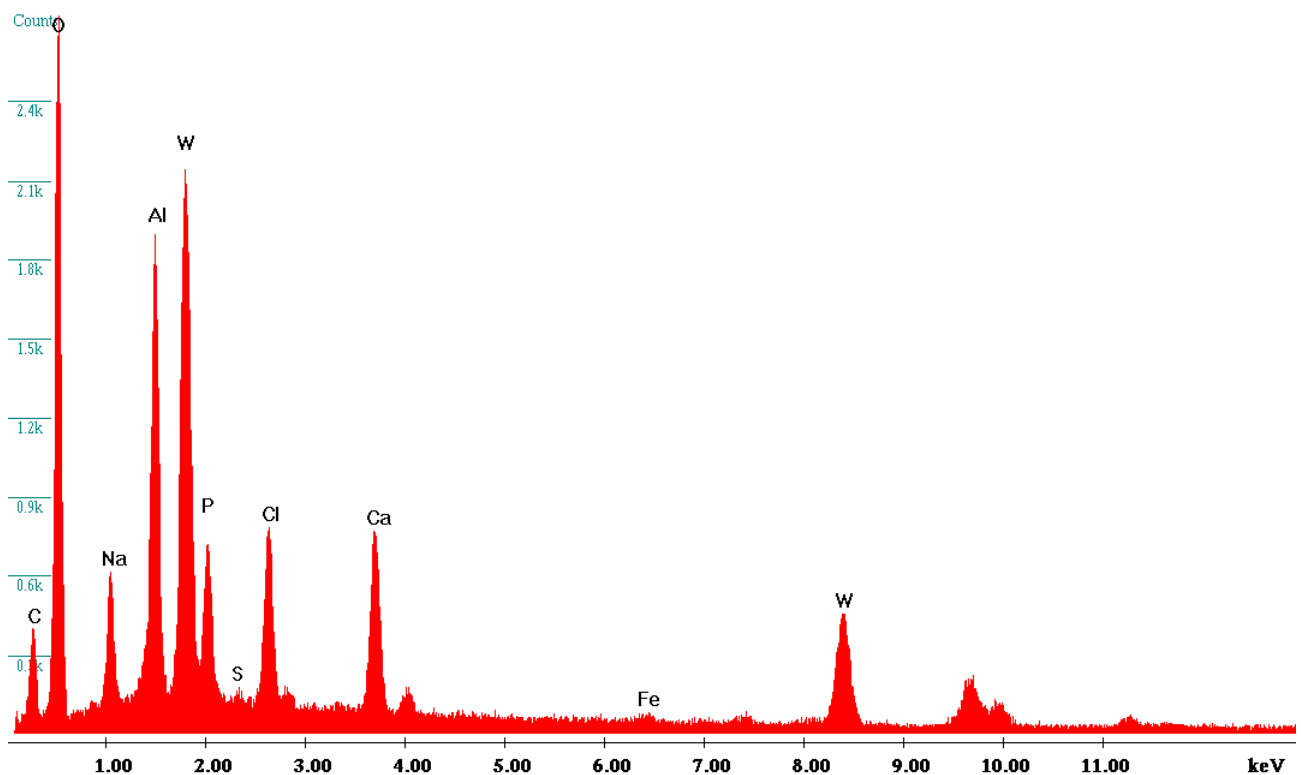
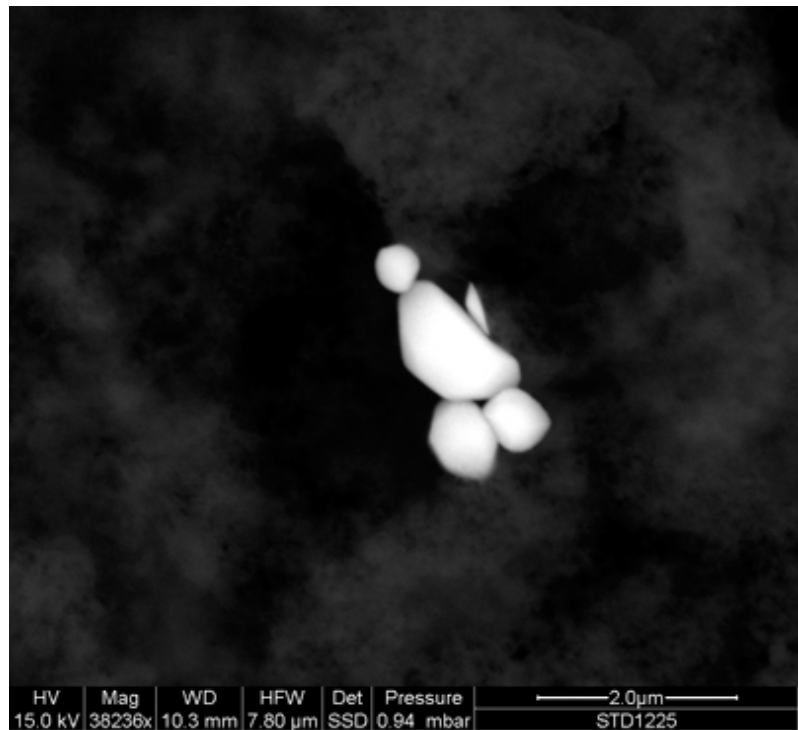


Image 5. The image shows the previous image at higher magnification (38236x) where 5 particles (0.3 – 1.5 microns) are visible. The debris are composed of Oxygen, Tungsten, Aluminum, Phosphorous, Sodium, Chlorine, Calcium, Carbon, Sulfur, Iron.

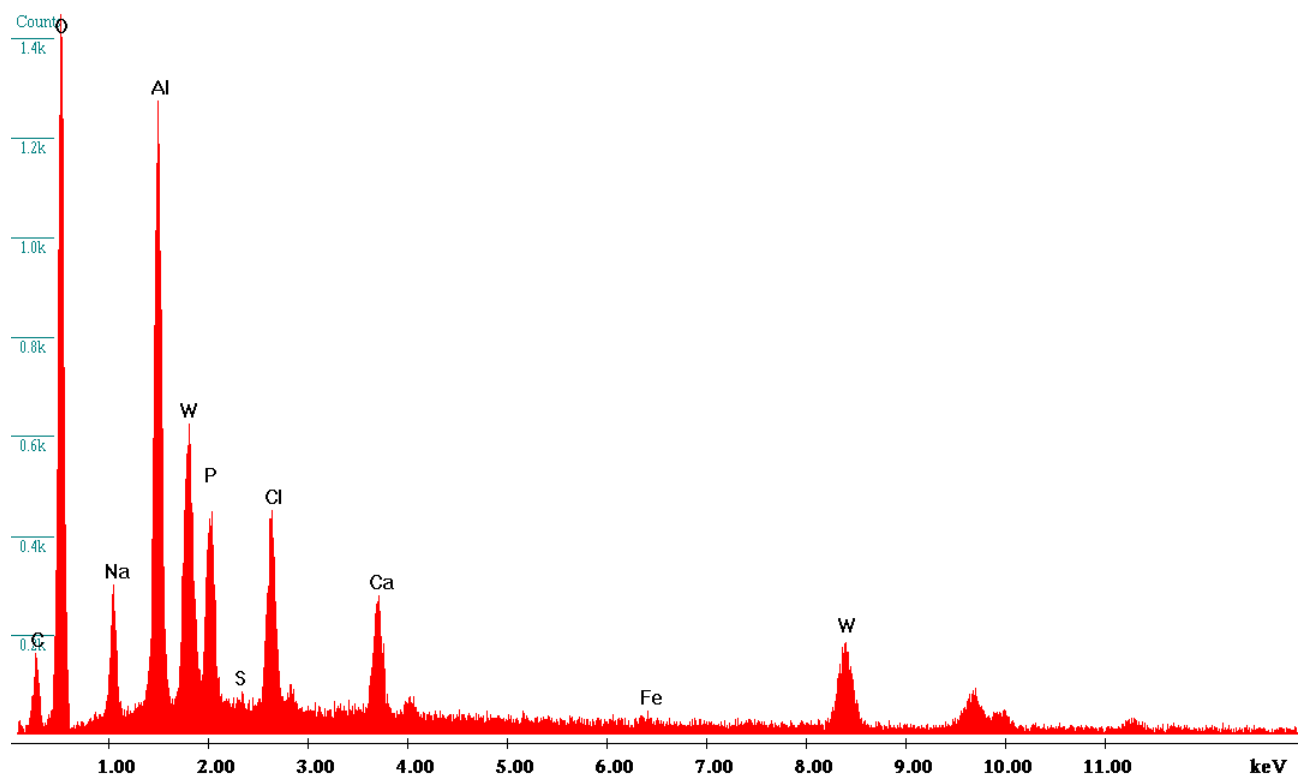
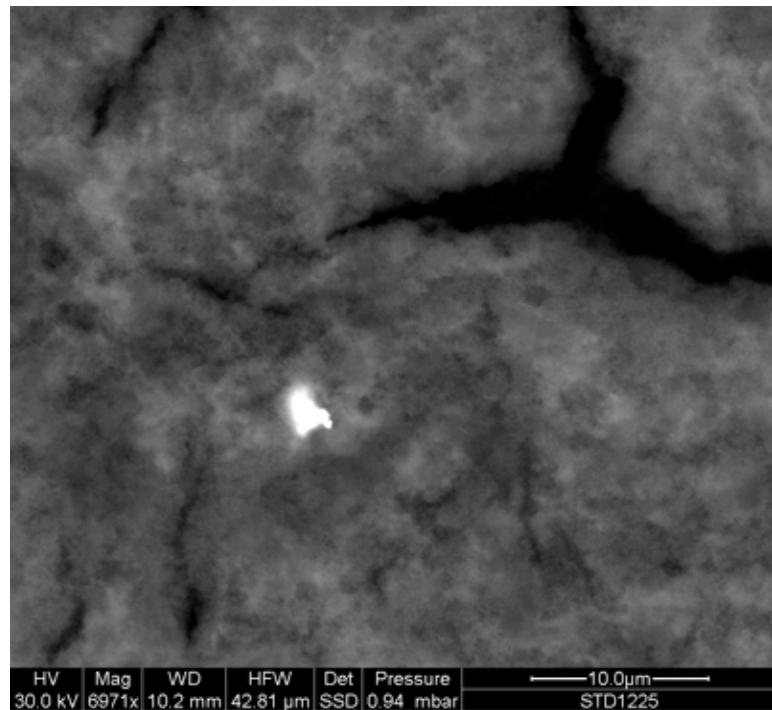


Image 6. The image (6971x) shows a 4-micron cluster of particles. The composition is Oxygen, Aluminum, Tungsten, Phosphorous, Chlorine, Sodium, Calcium, Sulfur, Iron. Qualitatively the same as the one of Analysis 5.

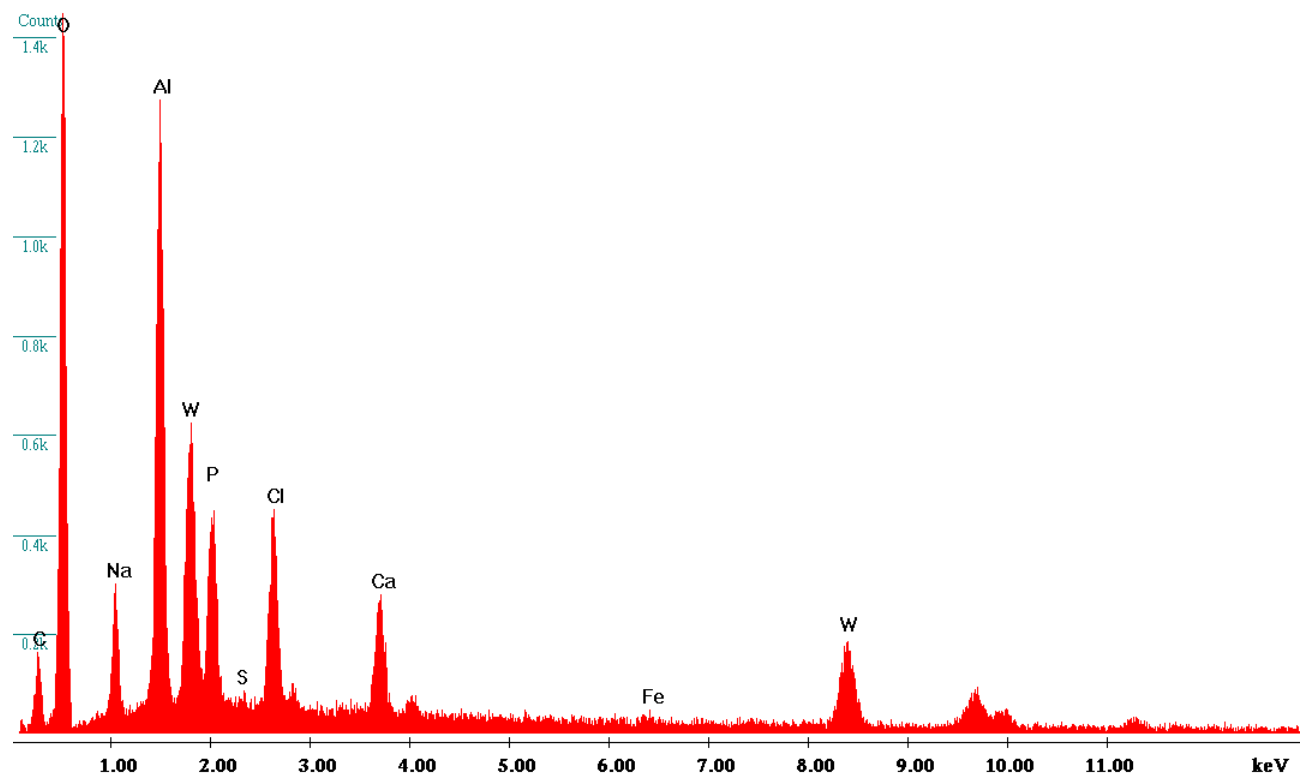
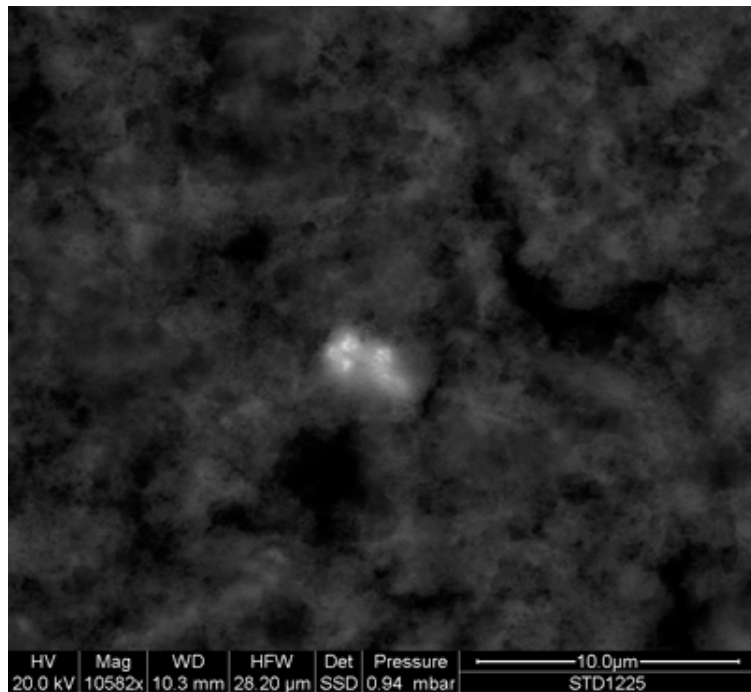


Image 7. The image shows another area of the vaccine droplet (10582x) where a 4-micron cluster of particles is visible. The qualitative composition of Oxygen, Aluminum, Tungsten, Phosphorous, Chlorine, Sodium, Calcium, Sulfur, Iron is the same as those of Analyses 5 and 6.

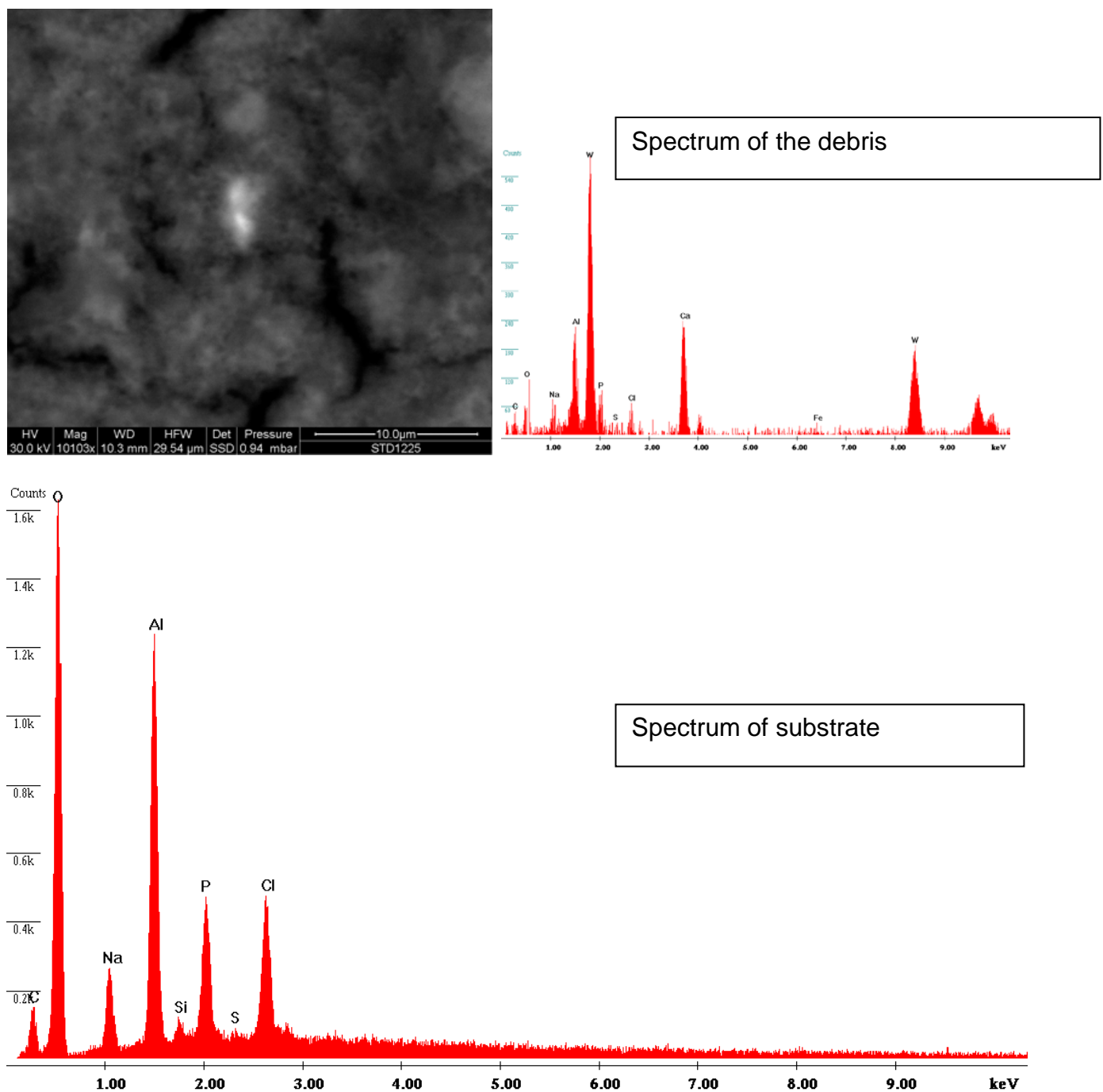


Image 8. The image shows at high magnification (10103x) a portion of the sample where a debris is visible. The EDS spectra show the debris chemistry (obtained by subtraction of the substrate signal) and that of the substrate (008std) . The debris is composed of Tungsten, Calcium, Iron, Calcium. The substrate (vaccine droplet) contains Oxygen-Aluminum-Chlorine-Phosphorus-Sodium-Silicon and Sulfur.

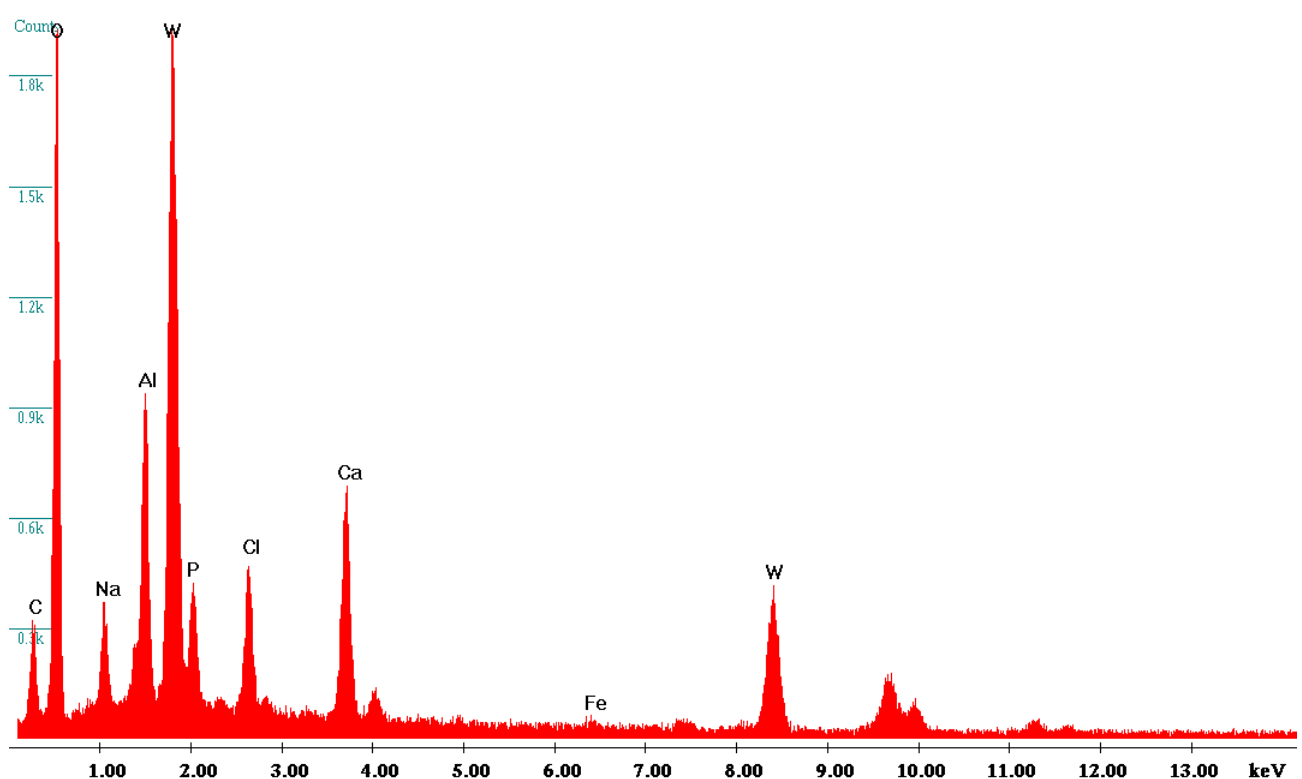
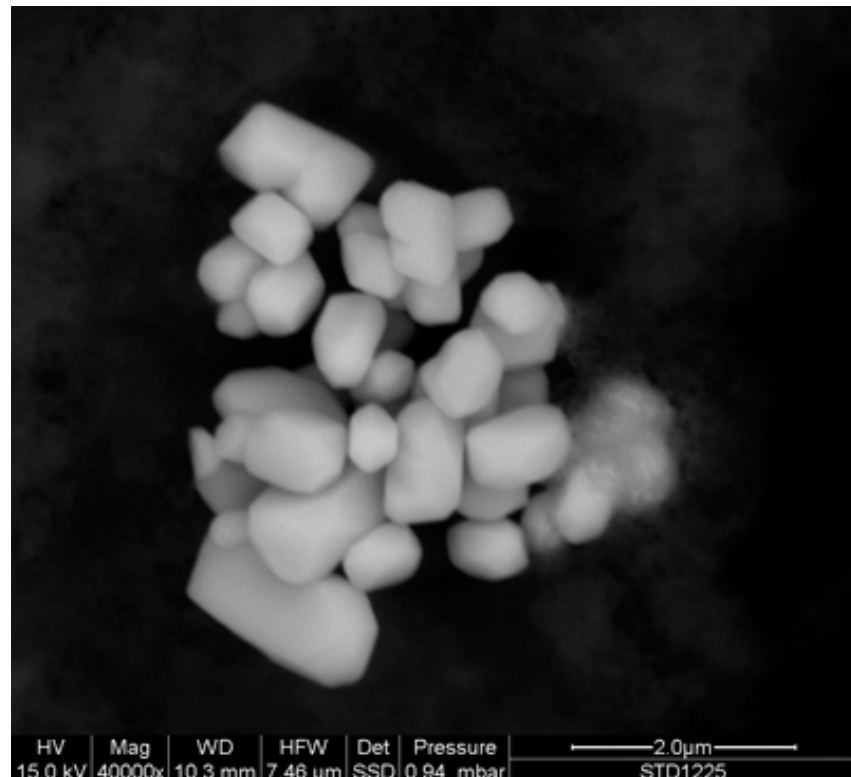


Image 9. A high-magnification (40000x) image of the Tungsten debris. A cluster of 0.3-1.8-micron particles is visible whose qualitative composition is the same as the one of Analyses, 5, 6 and 7. The particles are mainly composed of Tungsten.

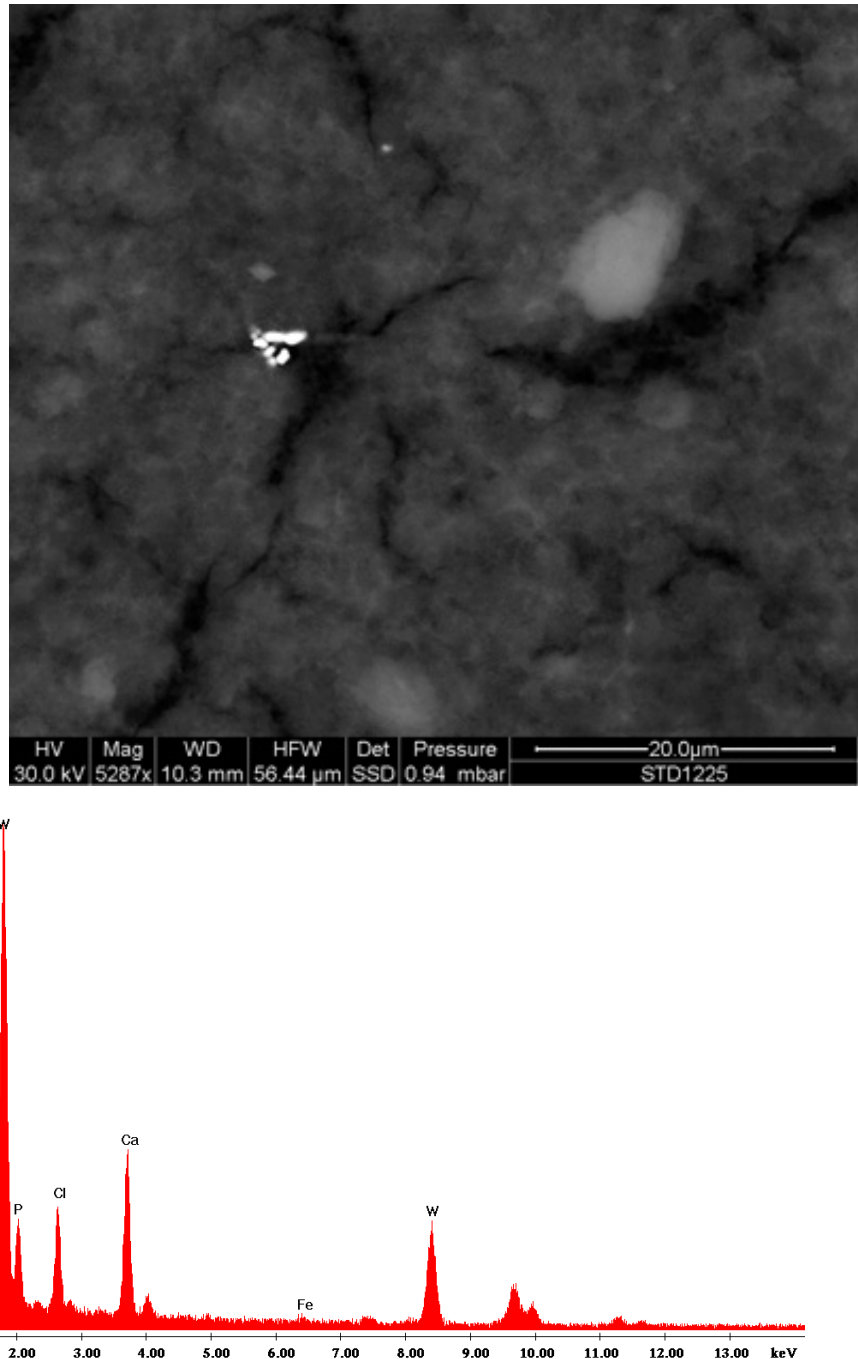


Image 10. The image shows further metallic debris mainly composed of Tungsten. (5287x). A section of the sample at high magnification (5287x) is shown where a few particles can be seen clustered.

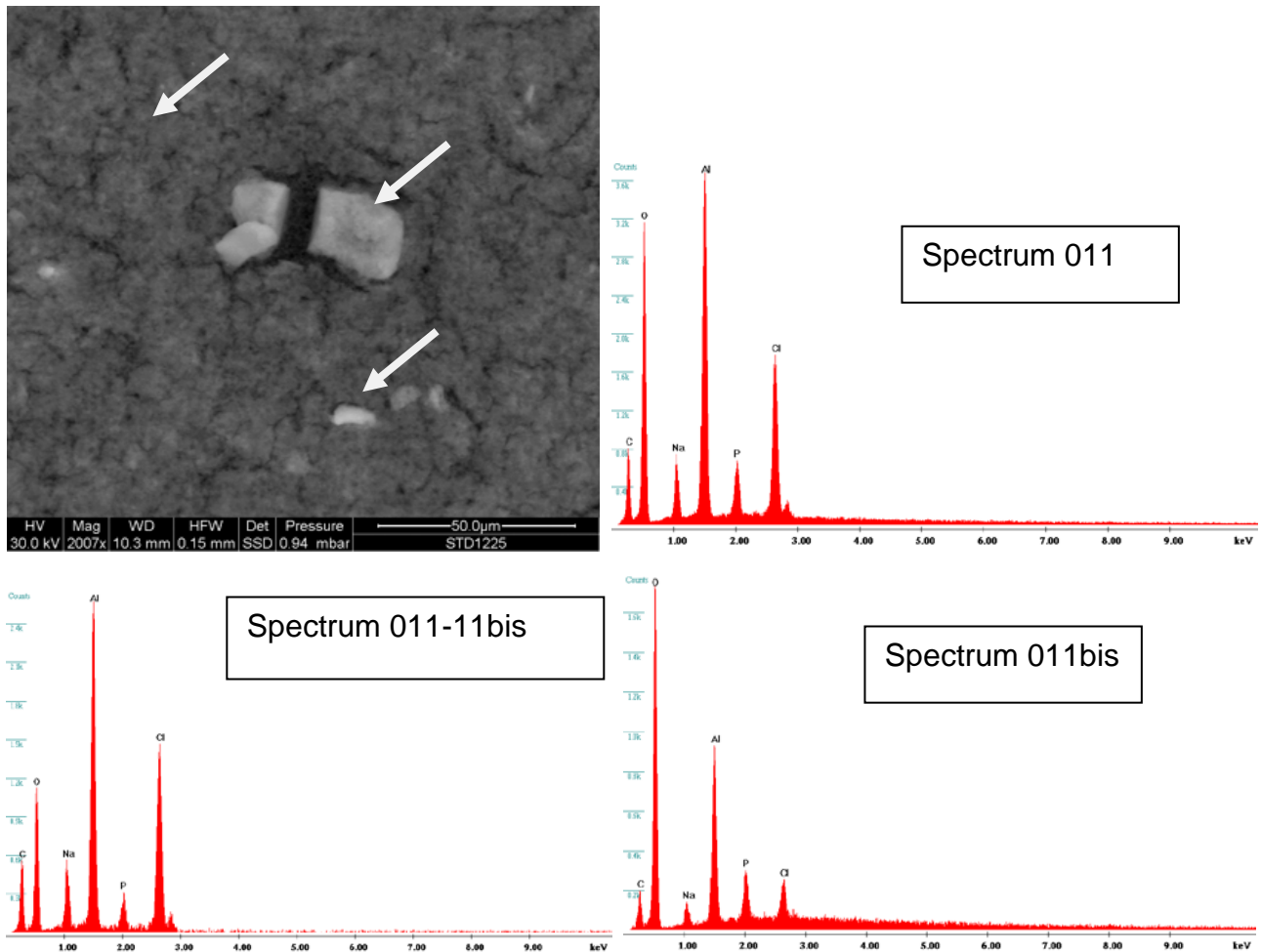


Image 11. The images show debris in the vaccine substrate (high magnification (2.007x)).

The spectra identify different zones.

011 - Alluminum, Oxygen, Chlorine, Carbon, Sodium, Phosphorous

011- 11 bis Aluminum, Chlorine, Oxygen, Carbon, Sodium, Phosphorus,

011bis Oxygen, Aluminum, Phosphorus, Chlorine, Carbon, Sodium

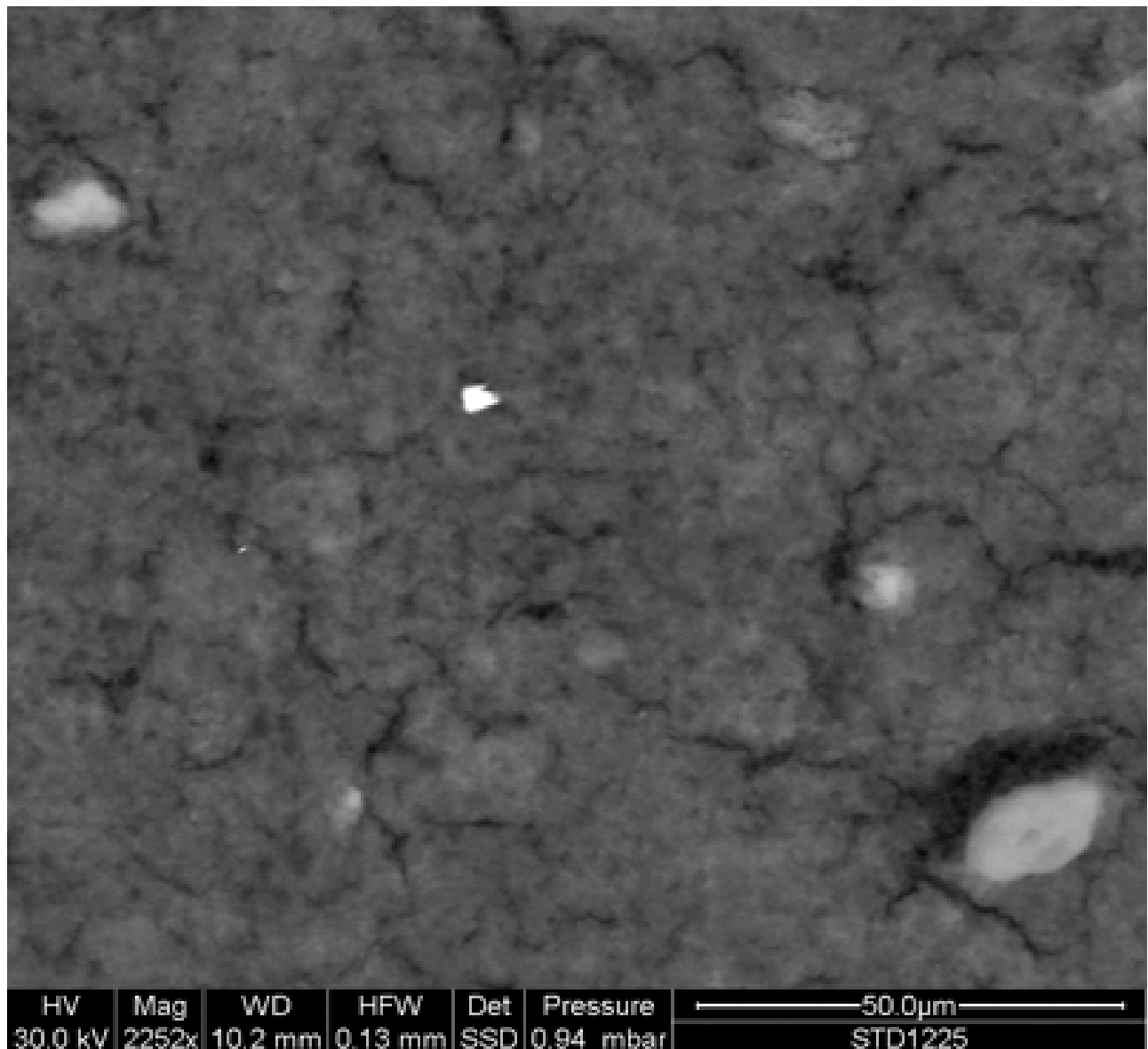


Image 12. The image shows an area of the sample at high magnification (2252x) where a bright debris is visible.

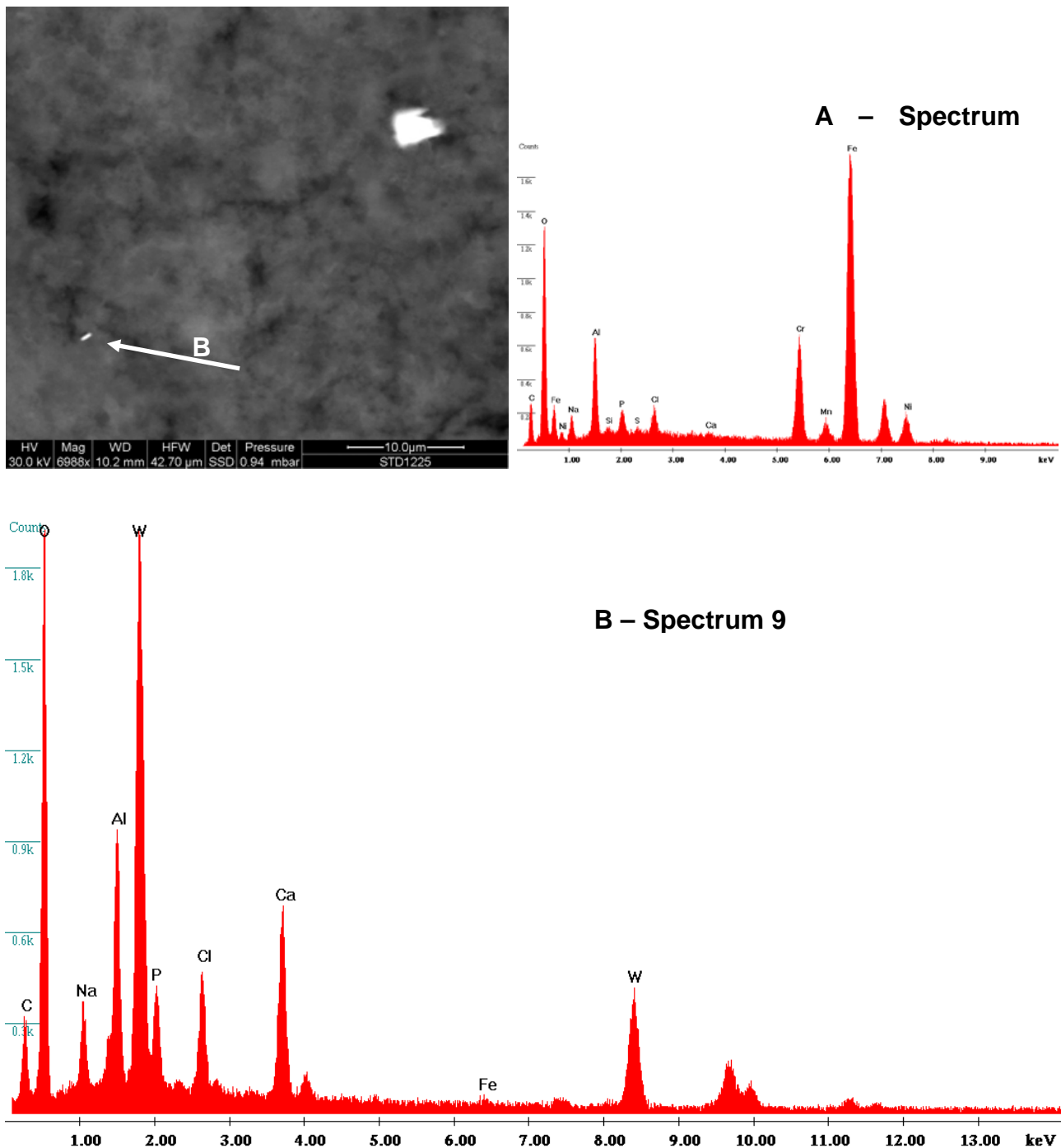


Image 13. The high-magnification (3.413x) photograph of the image of Analysis 12 shows an area where two particles, sized 5 and 0.8 microns respectively, can be seen. The 5-micron one (A) is composed of Iron, Oxygen, Aluminum, Chromium, Nickel, Chlorine, Phosphorous, Sodium, Silicon, Manganese, namely Stainless steel; while the 0.8-micron one (B) is composed of Oxygen, Tungsten, Aluminum, Calcium, Chlorine, Sodium, Phosphorous, Carbon and Iron, namely Tungsten as the other already identified..

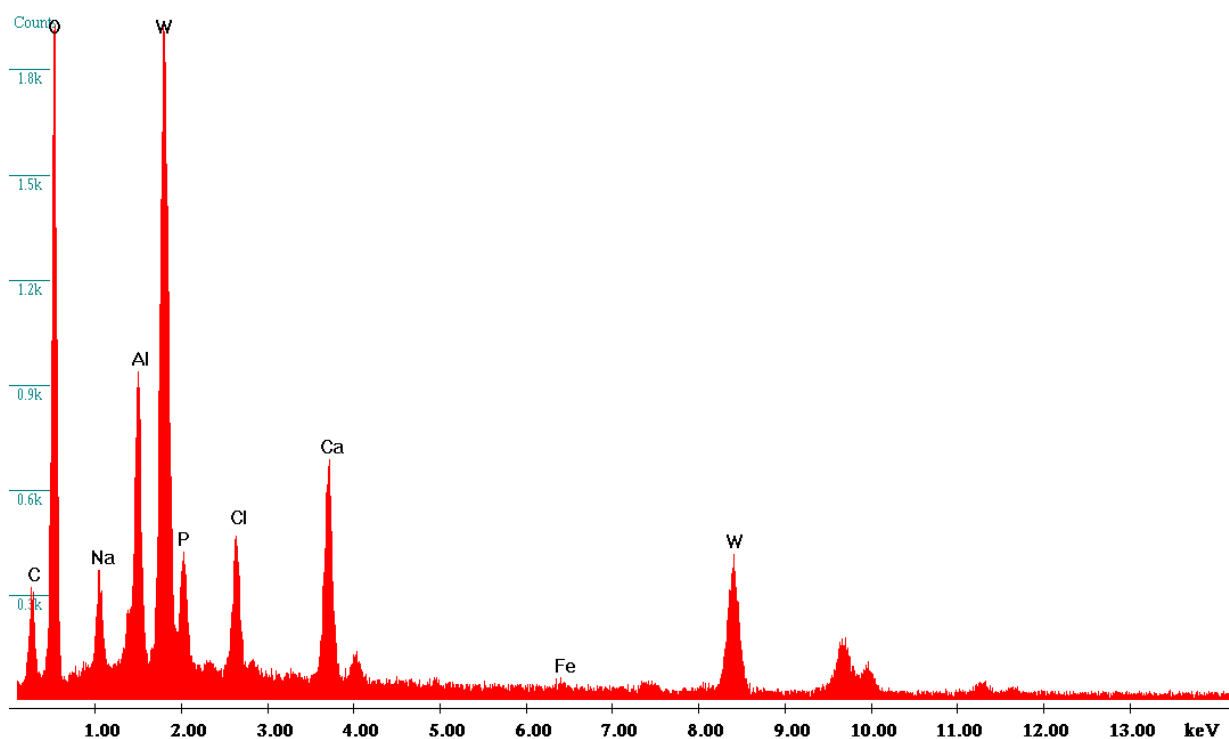
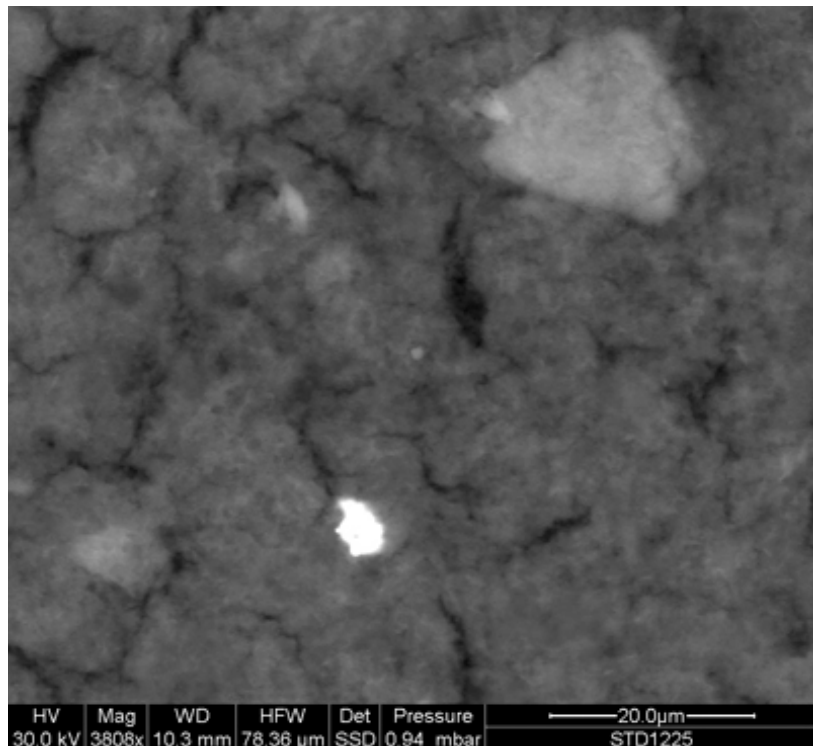


Image 14. The high-magnification (3808x) image shows a 7-micron detritus made of Oxygen, Tungsten, Aluminum, Calcium, Chlorine, Sodium, Phosphorous, Carbon and Iron. Again Tungsten is embedded in the Aluminum phosphatic precipitates.

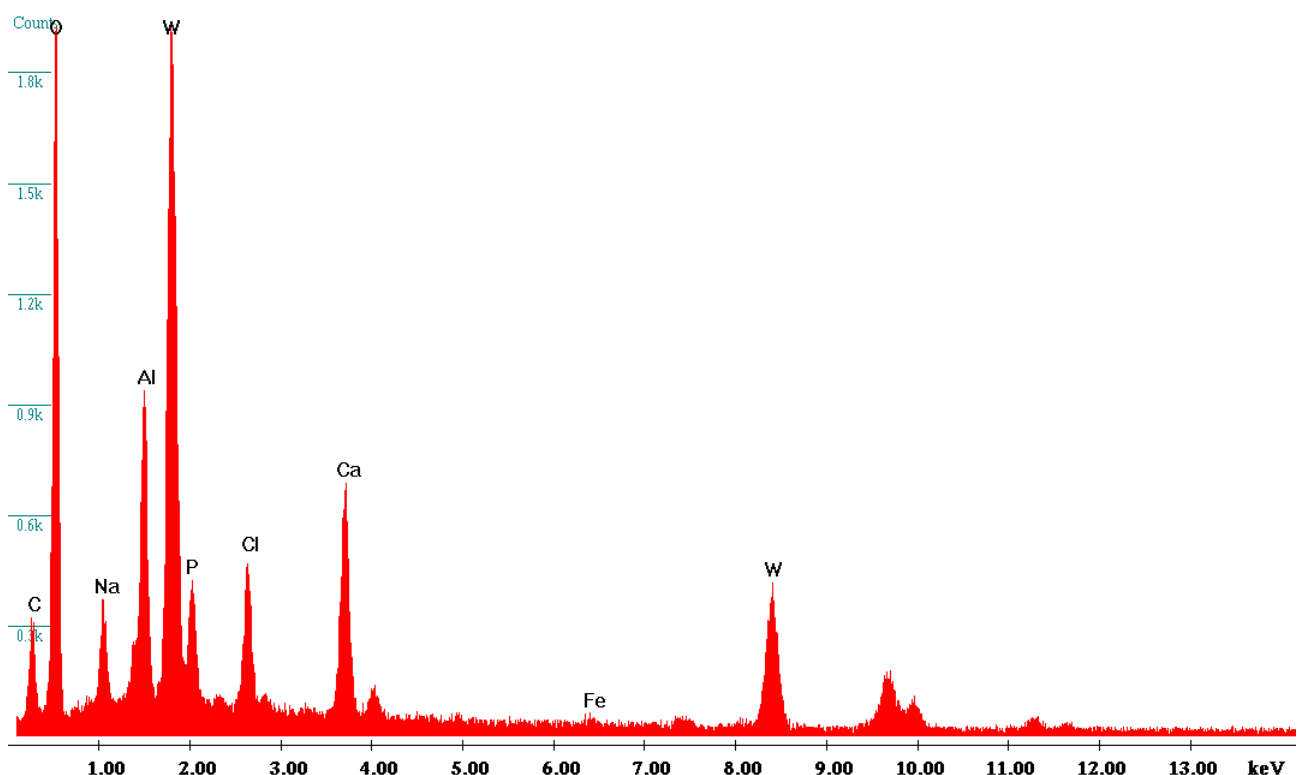
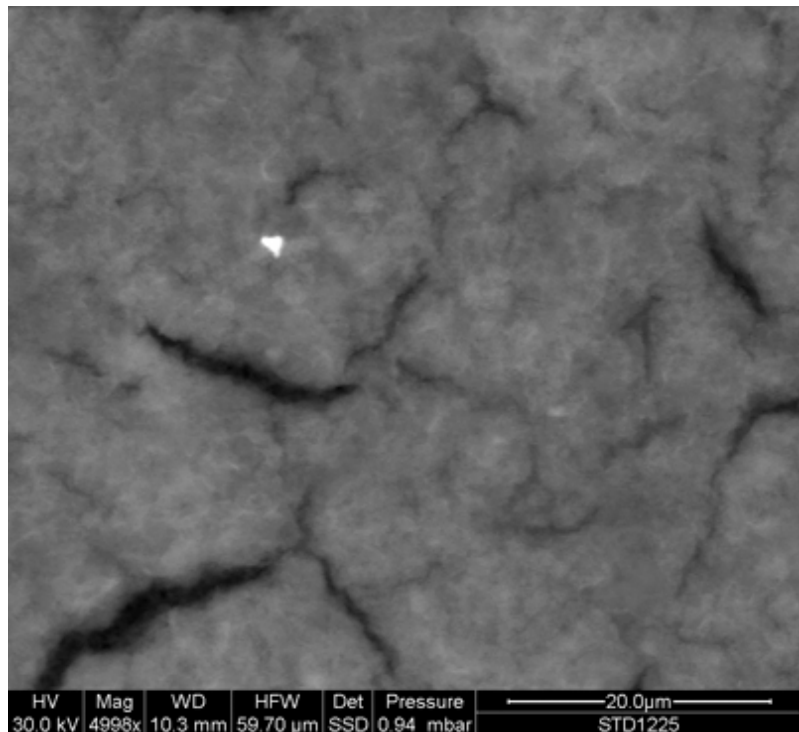


Image 15. A 1.5-micron particle is shown in the high-magnification (4998x) image. Its composition is Oxygen, Tungsten, Aluminum, Calcium, Chlorine, Sodium, Phosphorous, Carbon and Iron, a qualitative combination often observed throughout the sample.

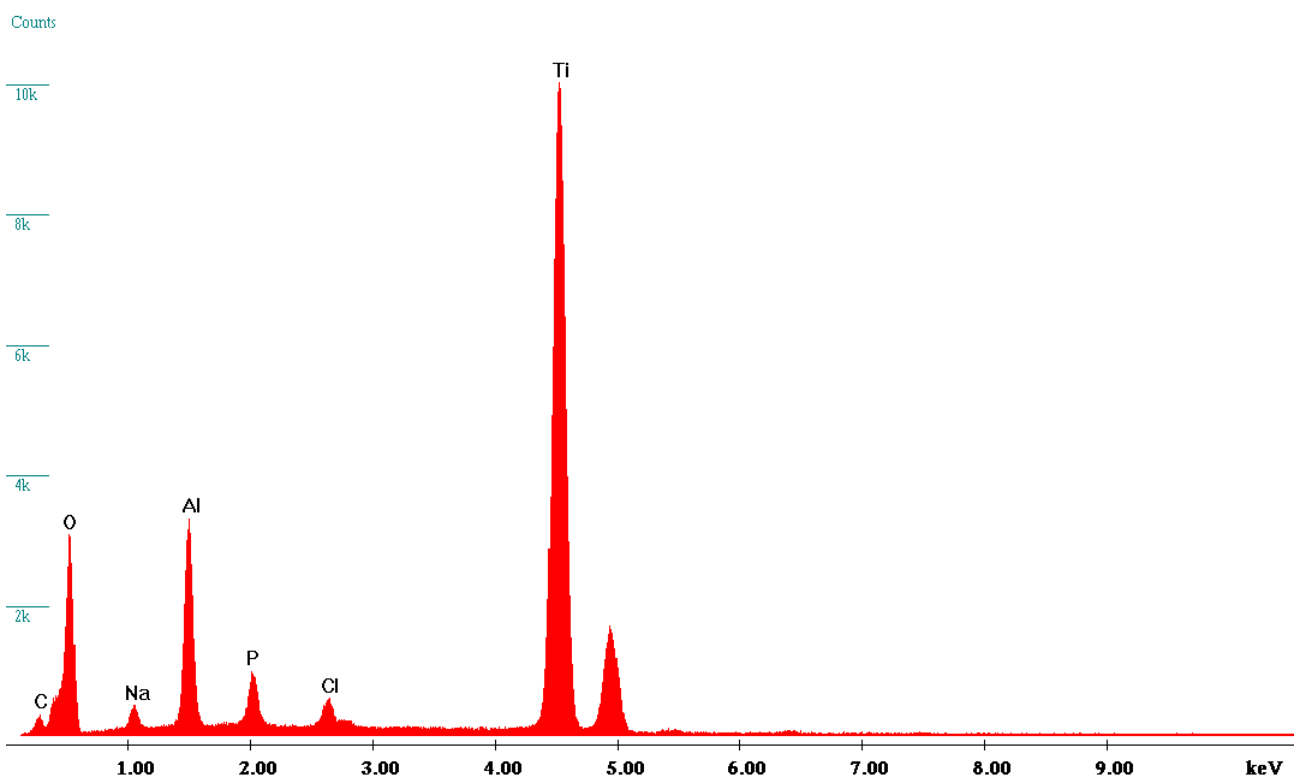
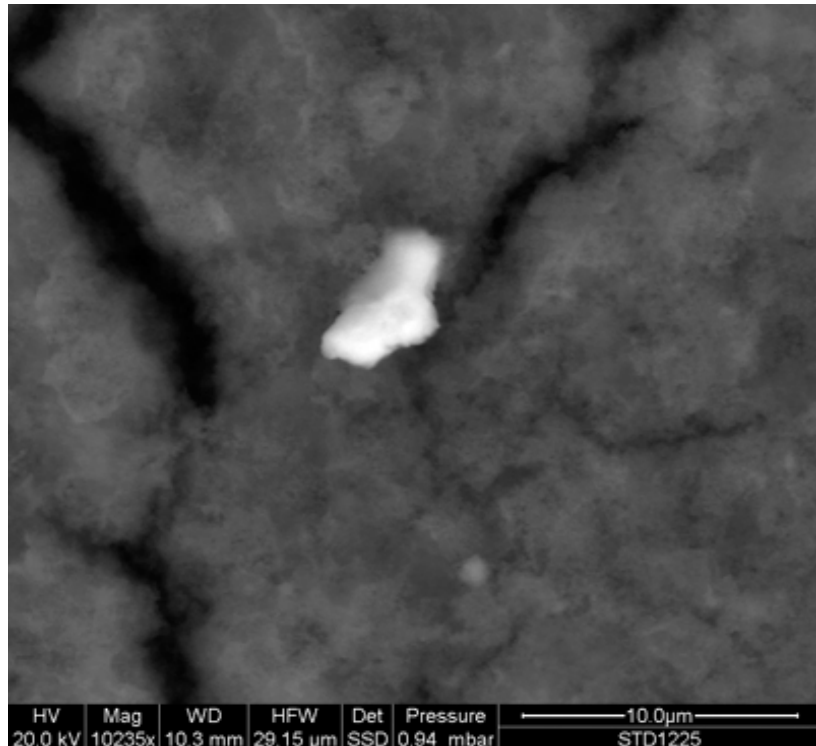


Image 16. The image shows a 5-micron particle (10235x) mainly composed of Titanium in the Aluminum background.

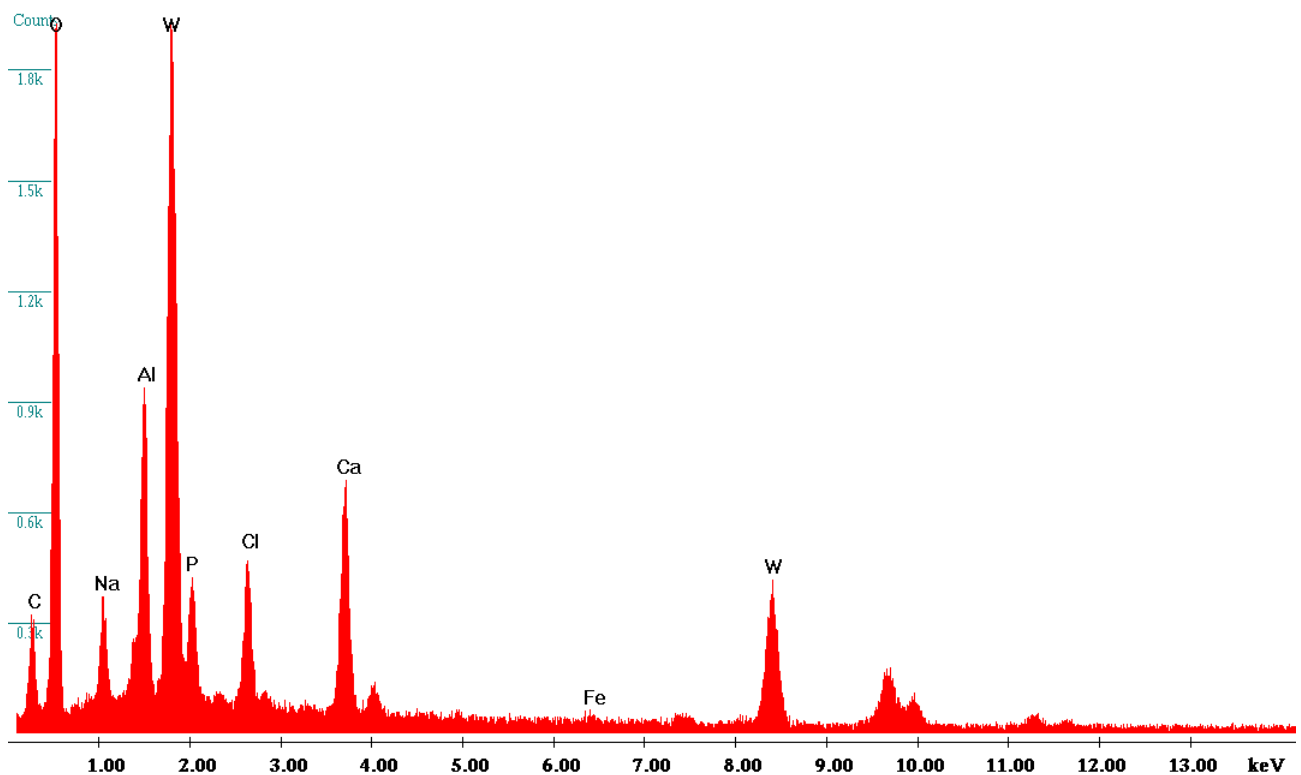
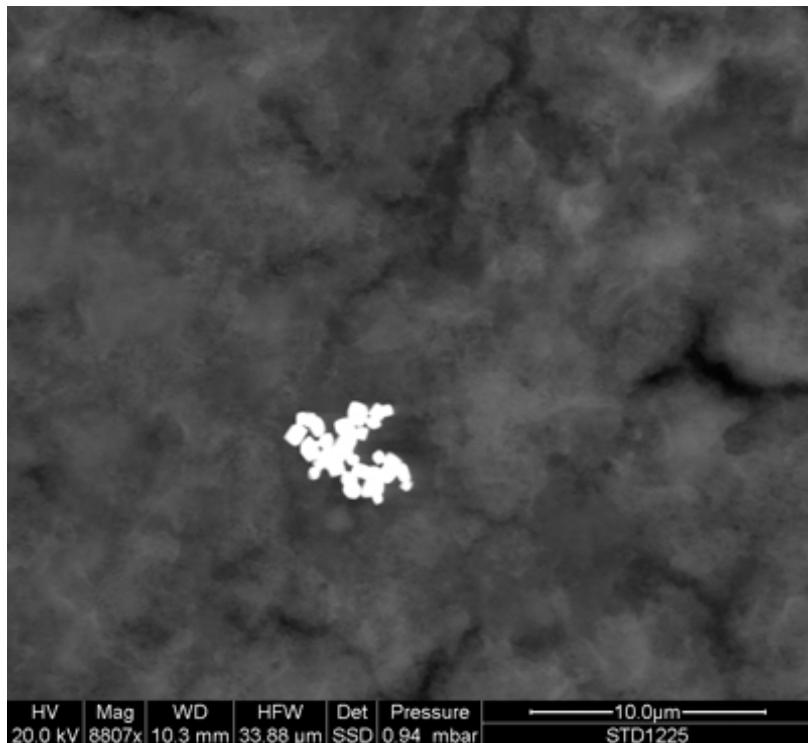


Image 17. Cluster of cubic particles, (8807x) with a size below 0.5 microns is shown. The composition of the particles is Oxygen, Tungsten, Aluminum, Calcium, Chlorine, Sodium, Phosphorous, Carbon and Iron: the qualitative composition of many of the particles found in the sample.

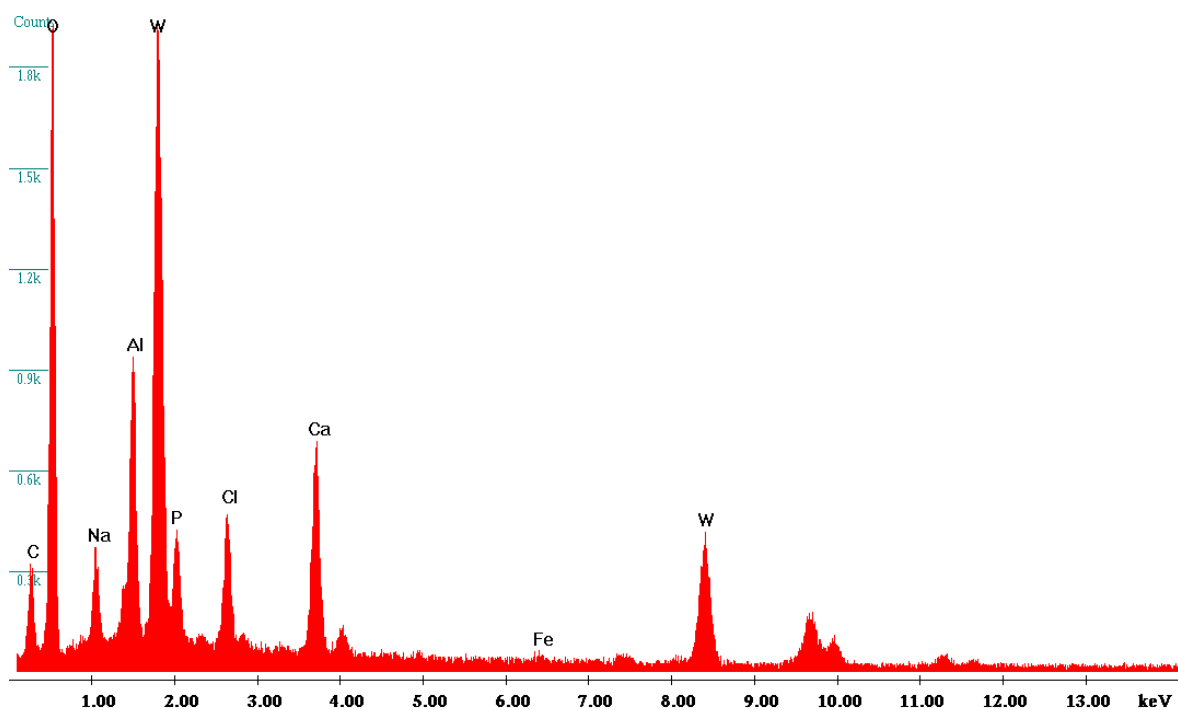
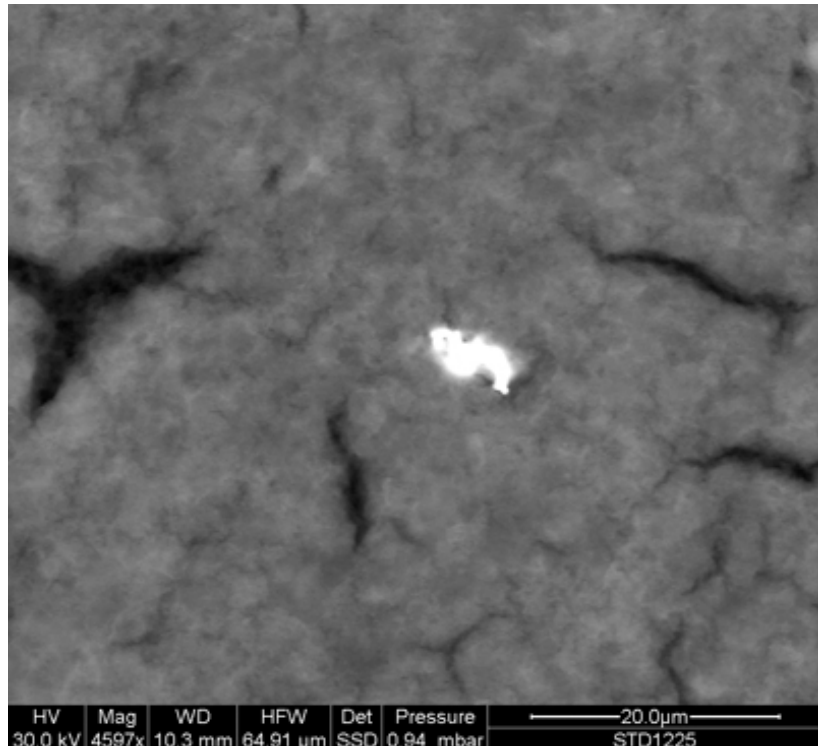


Image 18. Another aggregate of Tungsten debris is observed (4597x). Many of the particles composing it have a size smaller than 0.5 microns. The qualitative composition is the same as the one observed in many other particles in this specimen: Oxygen, Tungsten, Aluminum, Calcium, Chlorine, Sodium, Phosphorous, Carbon and Iron.

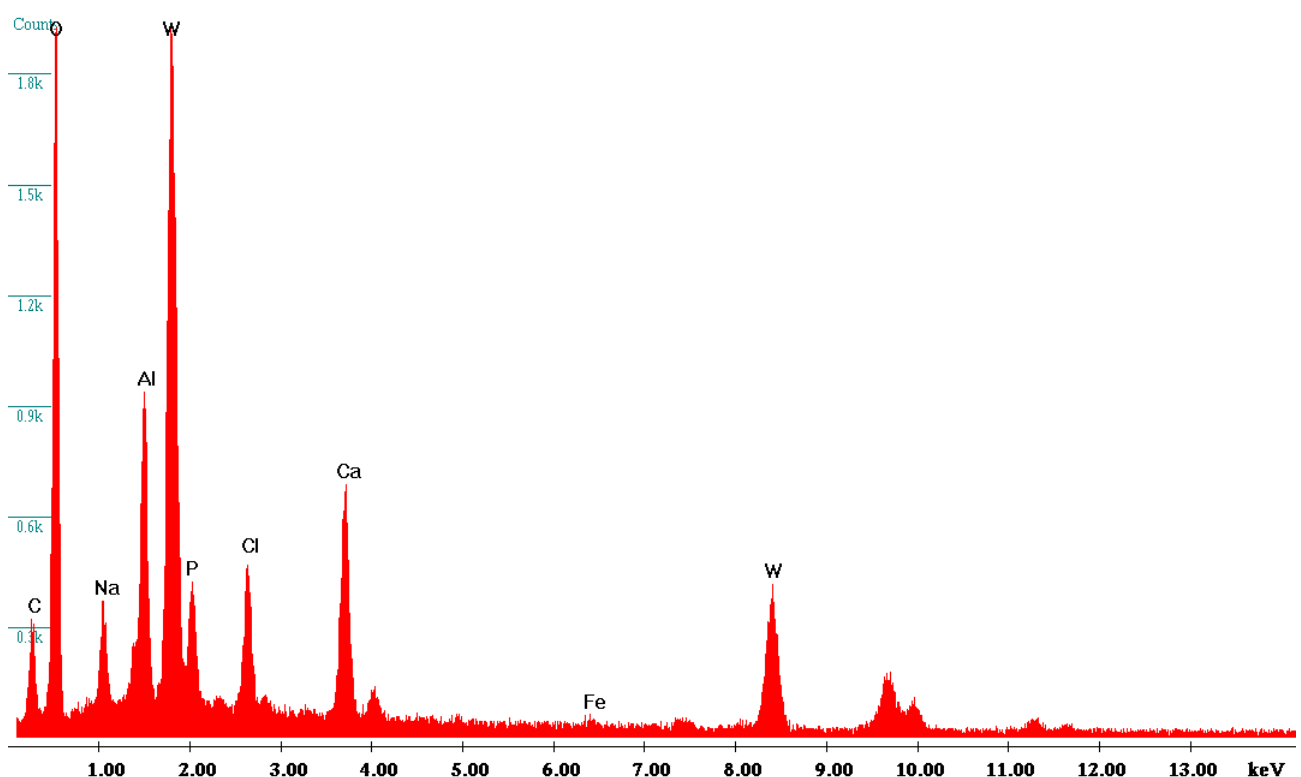
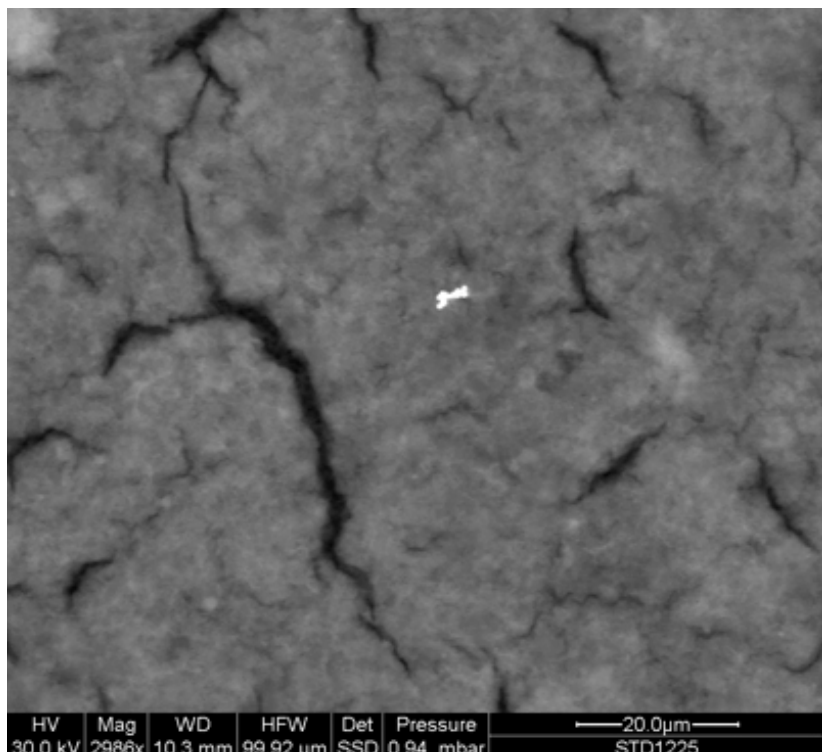
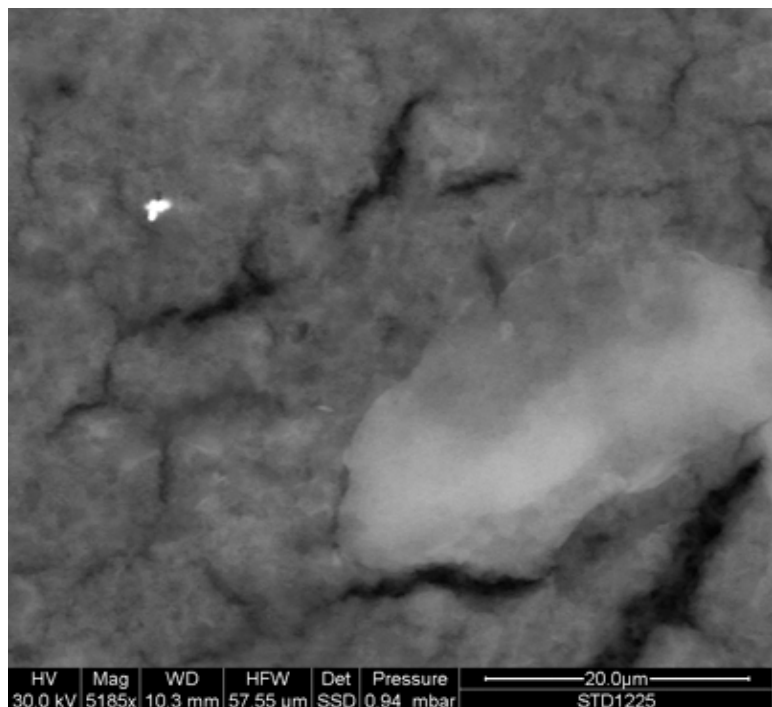


Image 19. A debris composed of smaller particles seen at high magnification (2986x) shows the much detected qualitative composition: Oxygen, Tungsten, Aluminum, Calcium, Chlorine, Sodium, Phosphorous, Carbon and Iron.



HV Mag WD HFW Det Pressure
30.0 kV 5185x 10.3 mm 57.55 µm SSD 0.94 mbar
STD1225

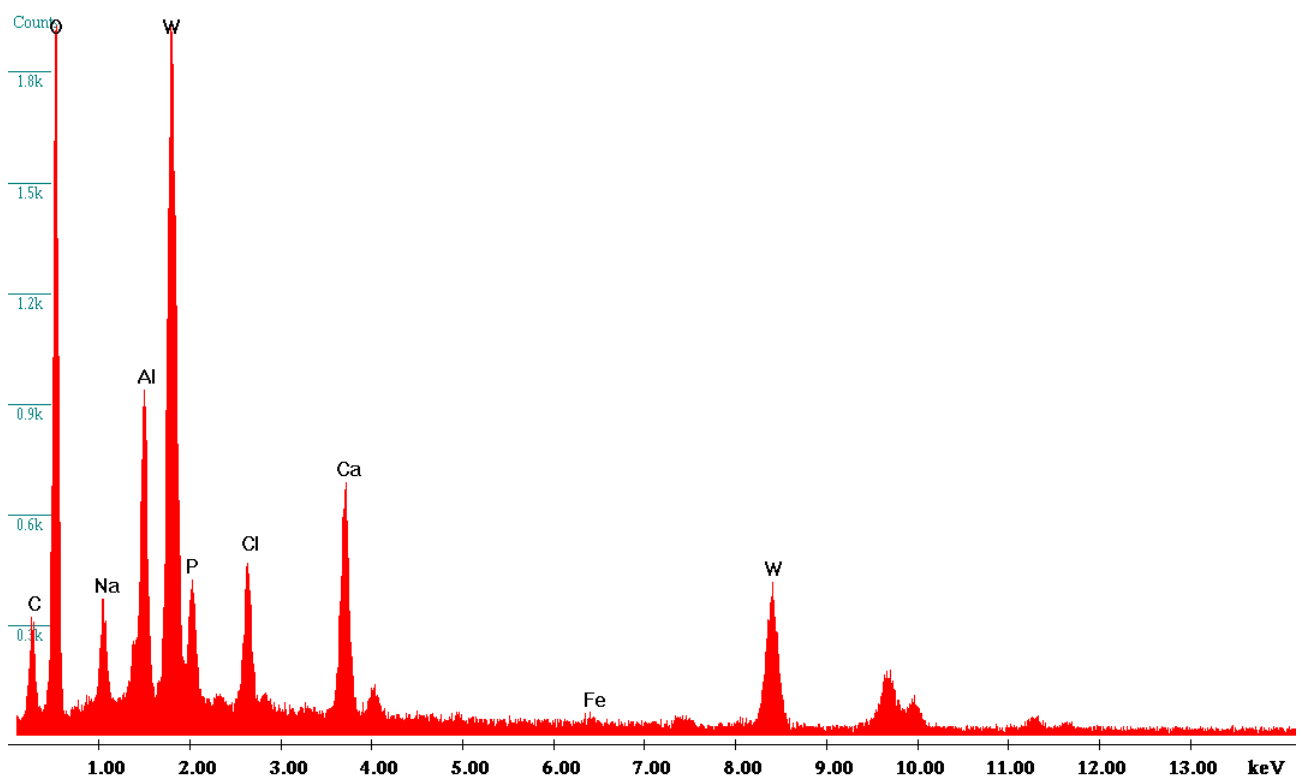


Image 20. At a magnification of 2986x, a debris sized below 1 micron and composed of much smaller particles can be seen. Its composition is qualitatively the same as very often detected in this sample: Oxygen, Tungsten, Aluminum, Calcium, Chlorine, Sodium, Phosphorous, Carbon and Iron.

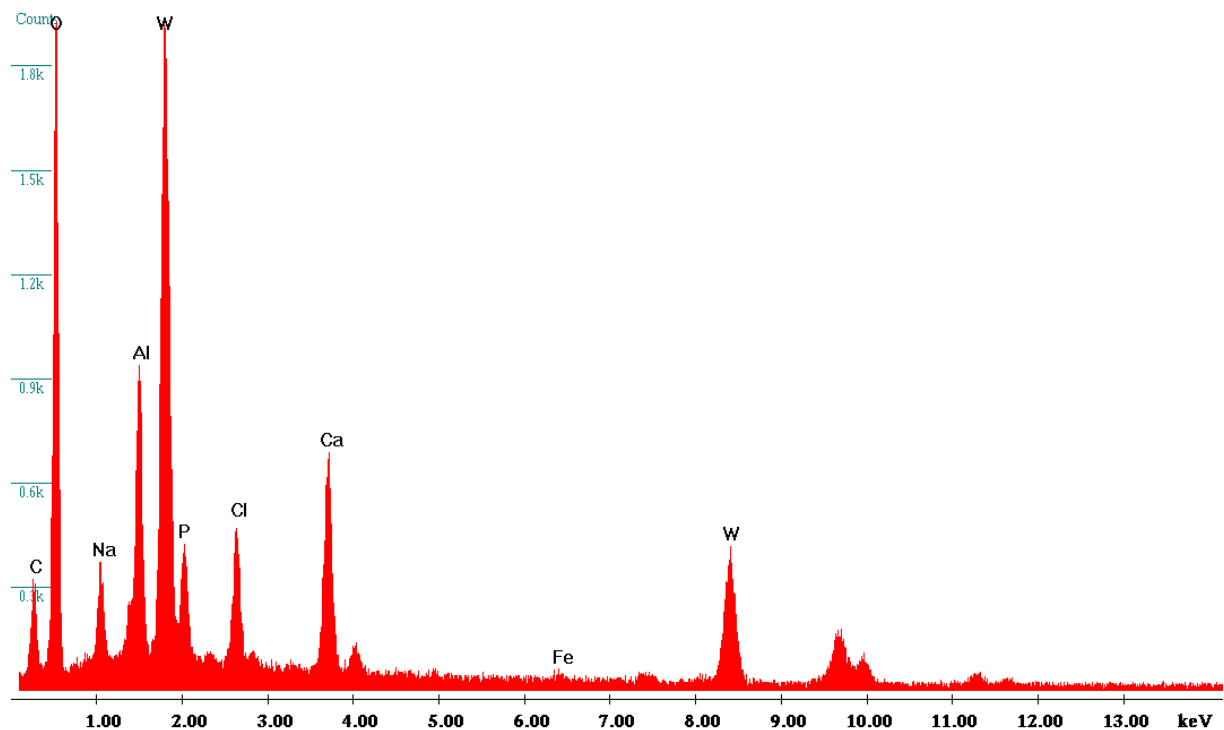
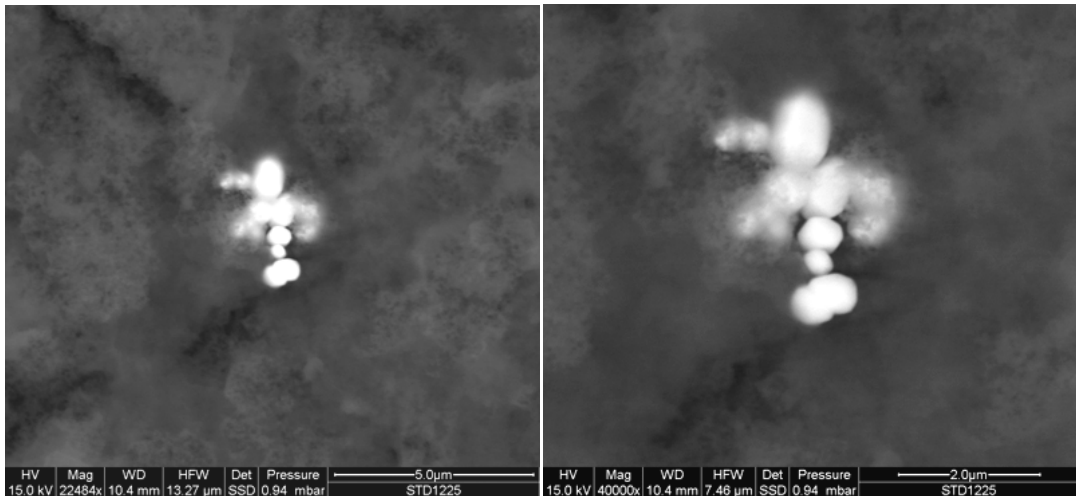


Image 21. At two different magnifications (22484x and 40000x), the images show an aggregate of Tungsten particles (sized 1 micron and below). The elemental composition is the “usual” one: Oxygen, Tungsten, Aluminum, Calcium, Chlorine, Sodium, Phosphorous, Carbon and Iron.

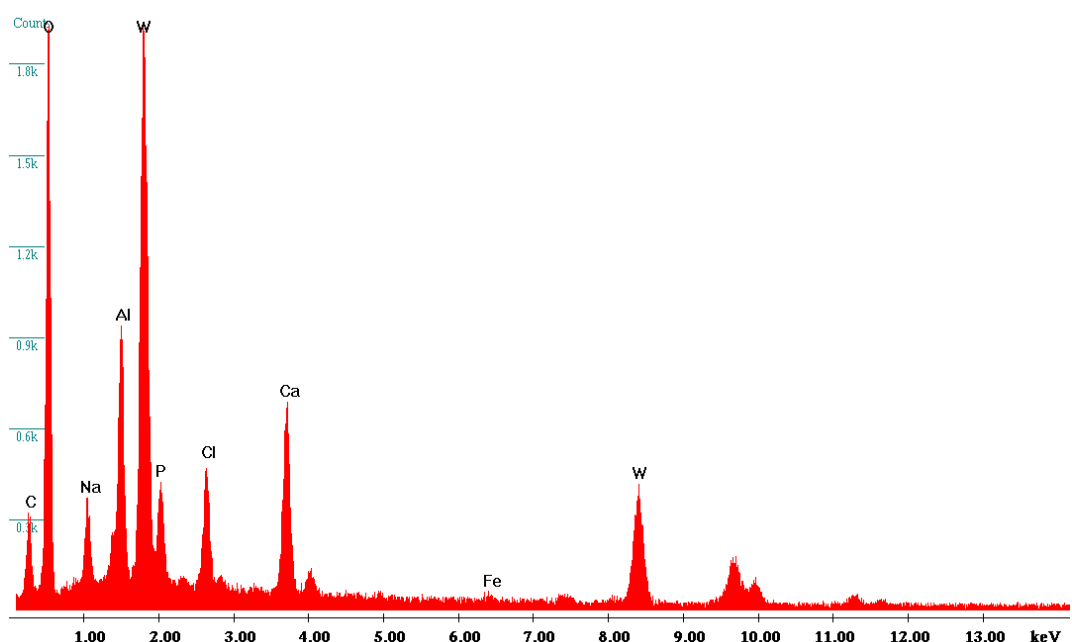
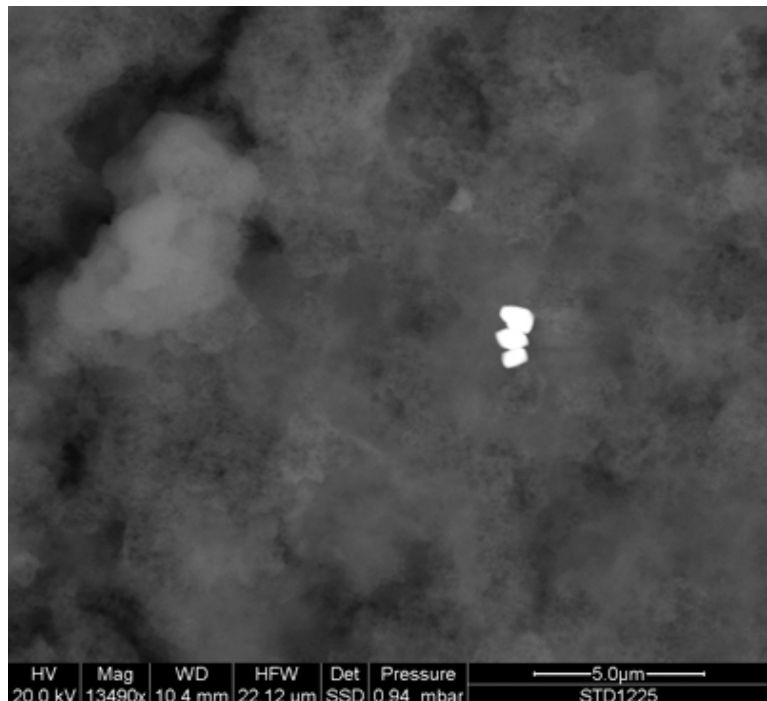
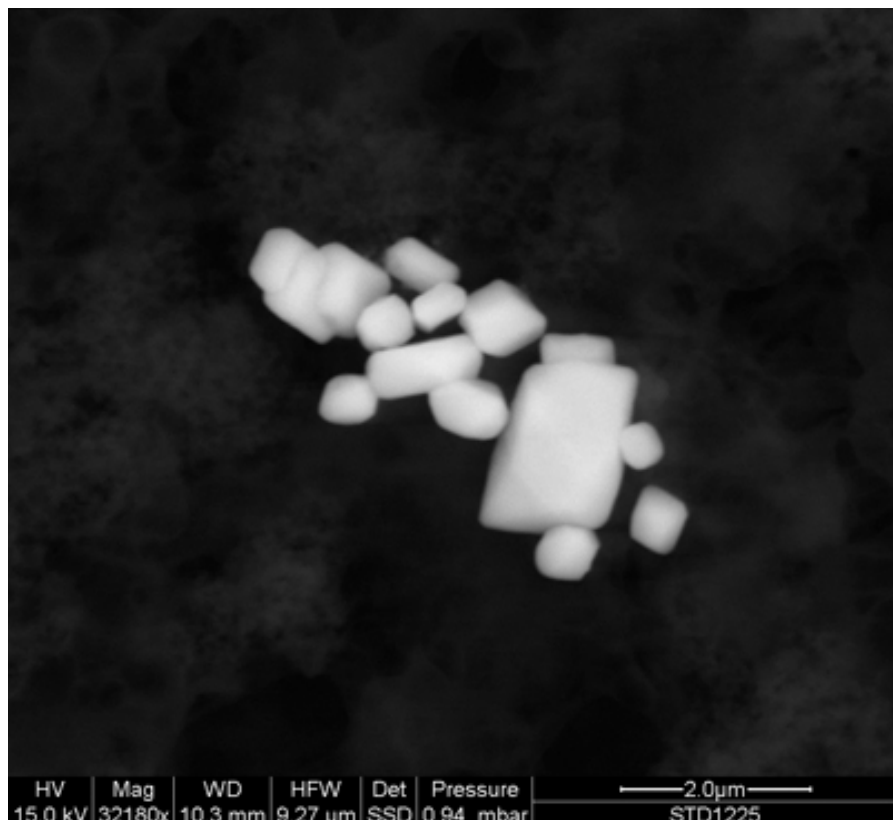


Image 22. At 13490x, three particles sized 1 micron can be seen. The composition is the same as that of many other particles observed in this sample: Oxygen, Tungsten, Aluminum, Calcium, Chlorine, Sodium, Phosphorous, Carbon and Iron.



HV | Mag | WD | HFW | Det | Pressure | ——————
15.0 kV | 32180x | 10.3 mm | 9.27 μm | SSD | 0.94 mbar | STD1225

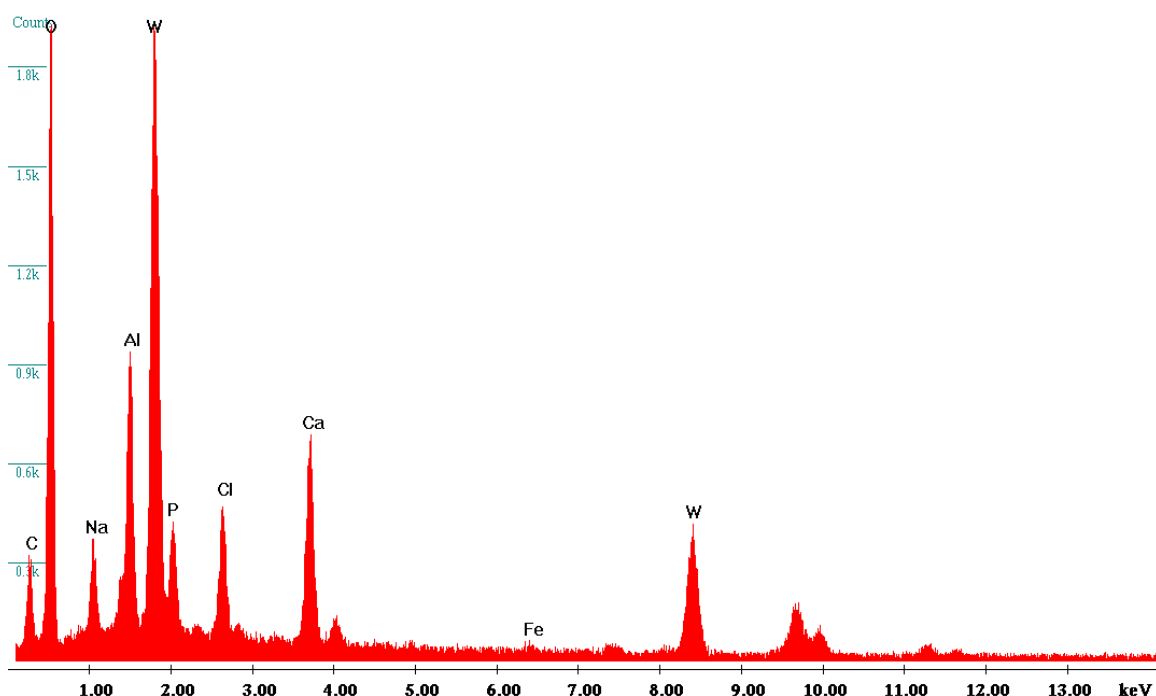


Image 23. The high-magnification (32180x) image shows an aggregate of Tungsten particles, sized 0.4-1 micron. Their composition is Oxygen, Tungsten, Aluminum, Calcium, Chlorine, Sodium, Phosphorous, Carbon and Iron.

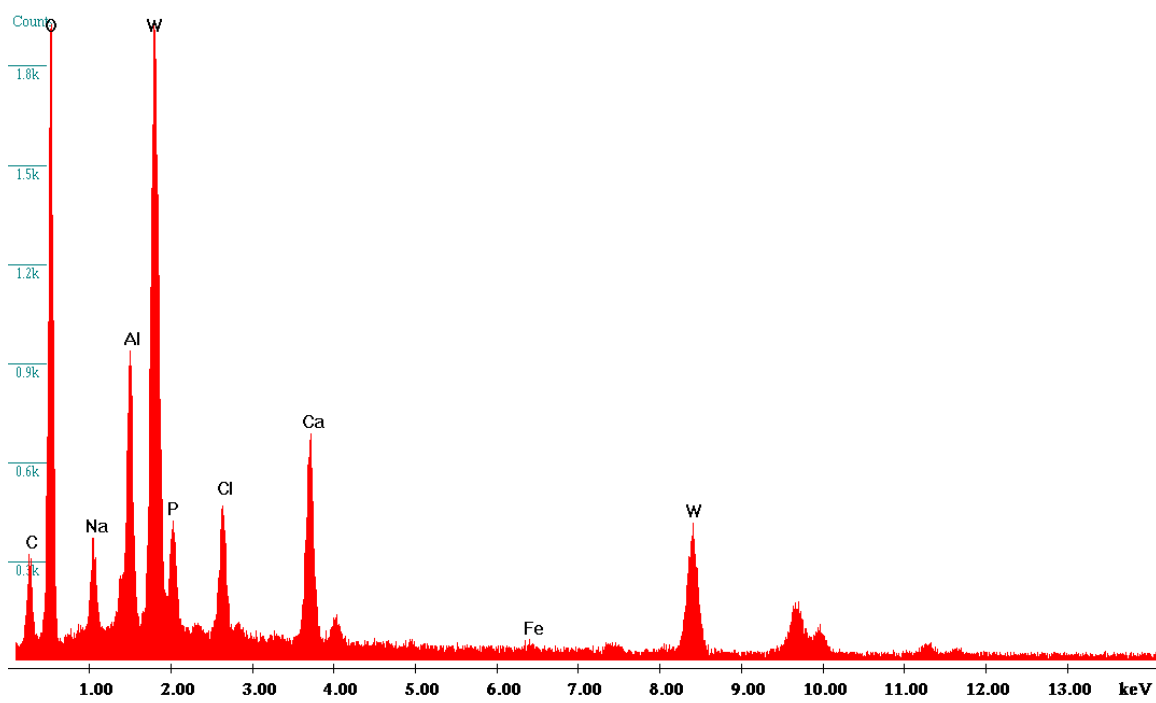
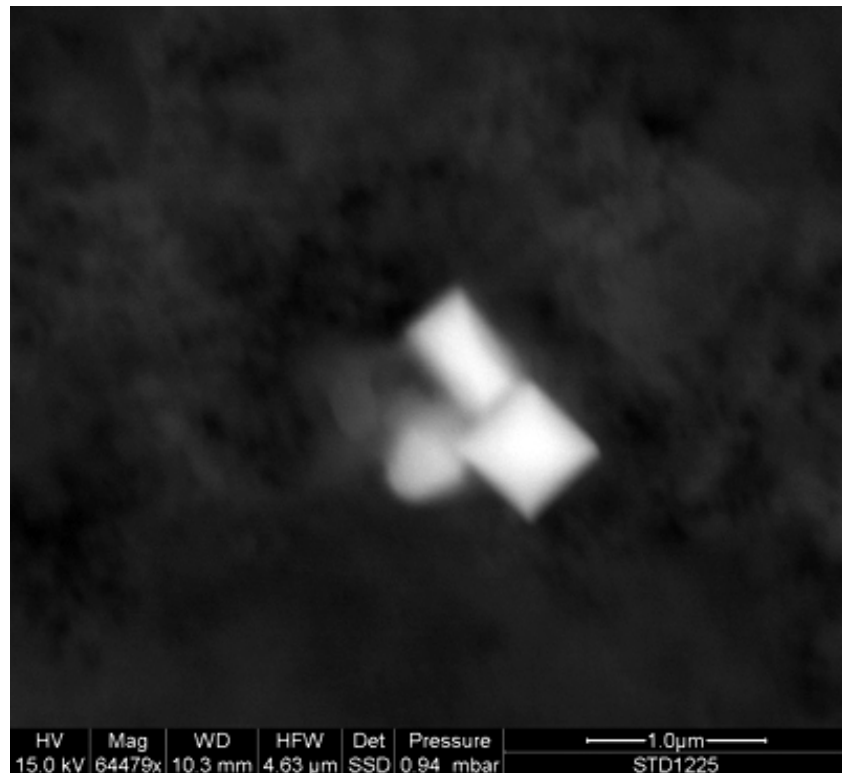


Image 24. At high magnification (64479x) particles with cubic morphology are visible. They have the same composition as many others found in this sample: Oxygen, Tungsten, Aluminum, Calcium, Chlorine, Sodium, Phosphorous, Carbon and Iron.

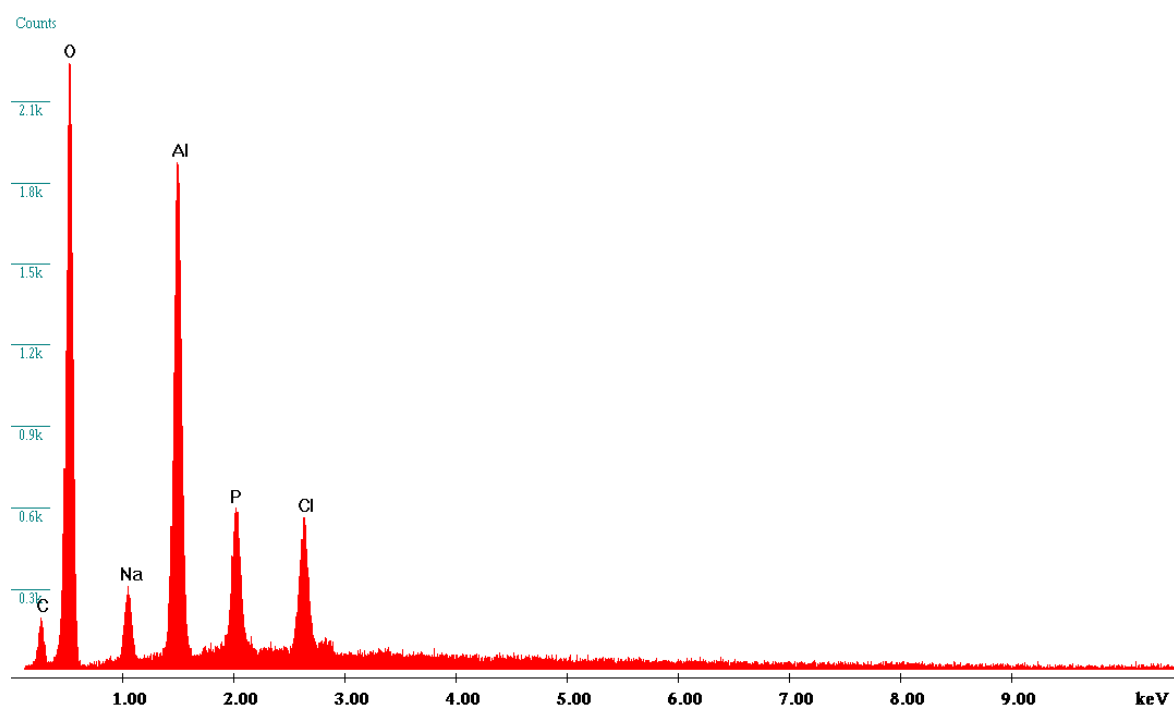
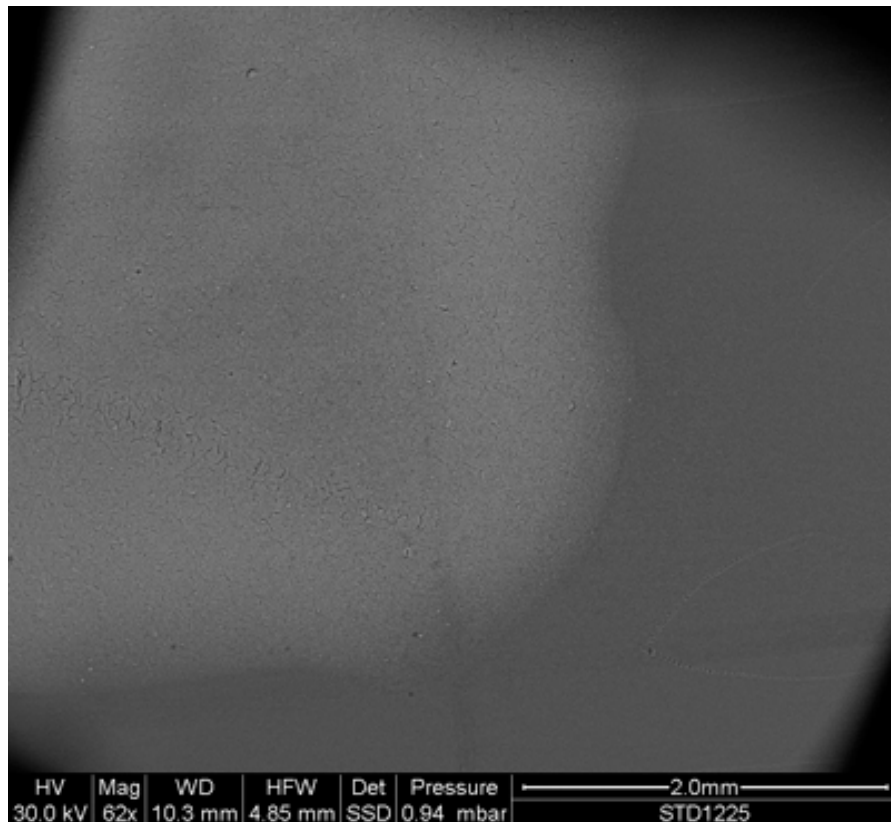


Image 25. The image shows another area of the vaccine droplet where only the Aluminum precipitates are present. The EDS spectrum identifies the drug's composition: Oxygen, Aluminum, Phosphorus, Chlorine, Sodium, Carbon.

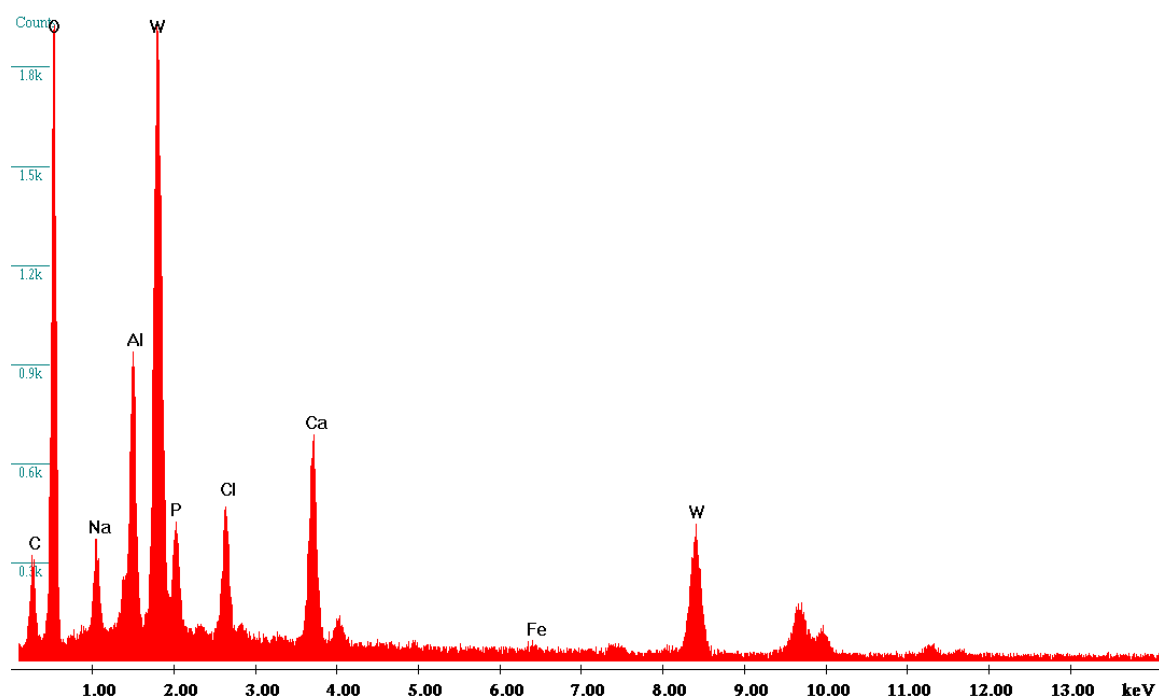
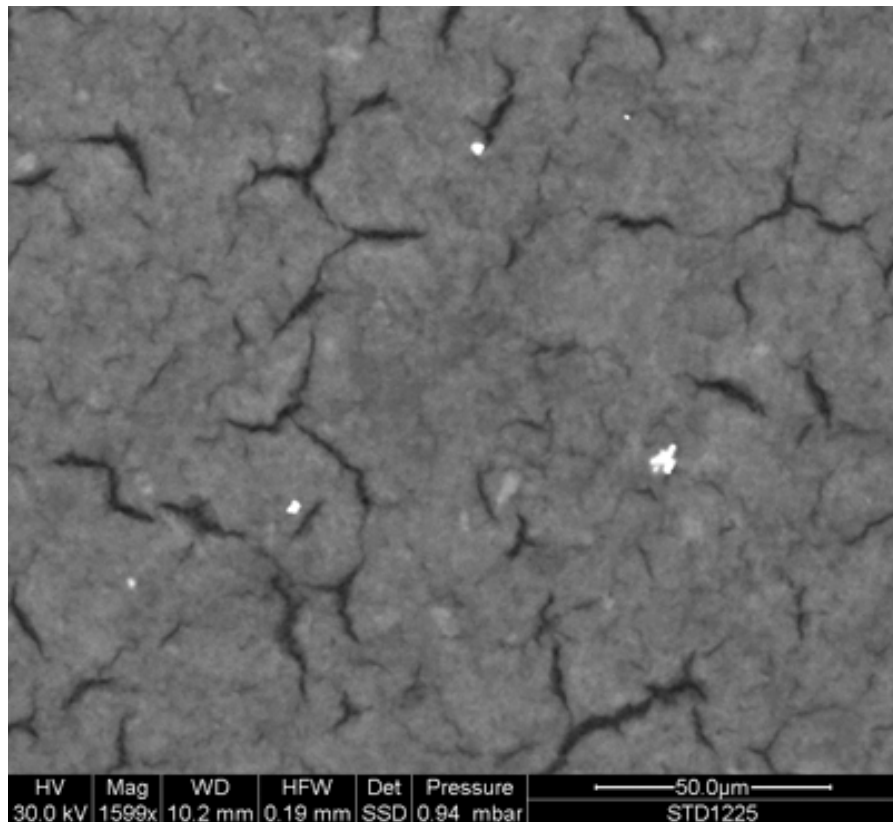
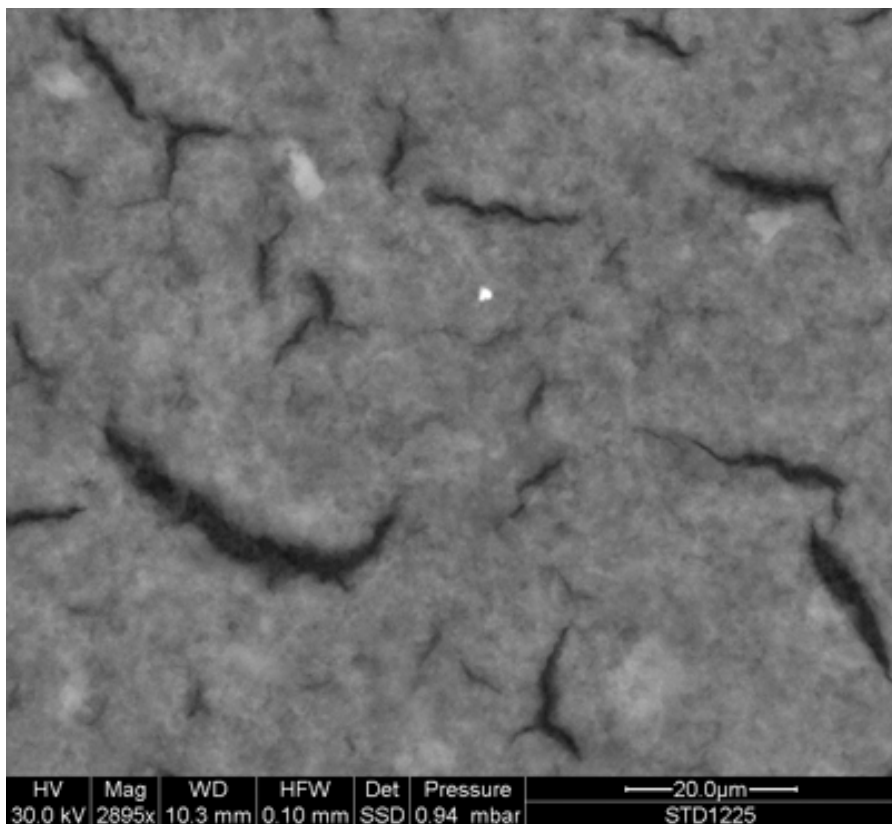


Image 26. The image shows other Tungsten-based debris (1599x).They are composed of Oxygen, Tungsten, Aluminum, Calcium, Chlorine, Sodium, Phosphorous, Carbon and Iron.



HV Mag WD HFW Det Pressure
30.0 kV 2895x 10.3 mm 0.10 mm SSD 0.94 mbar

—20.0μm—
STD1225

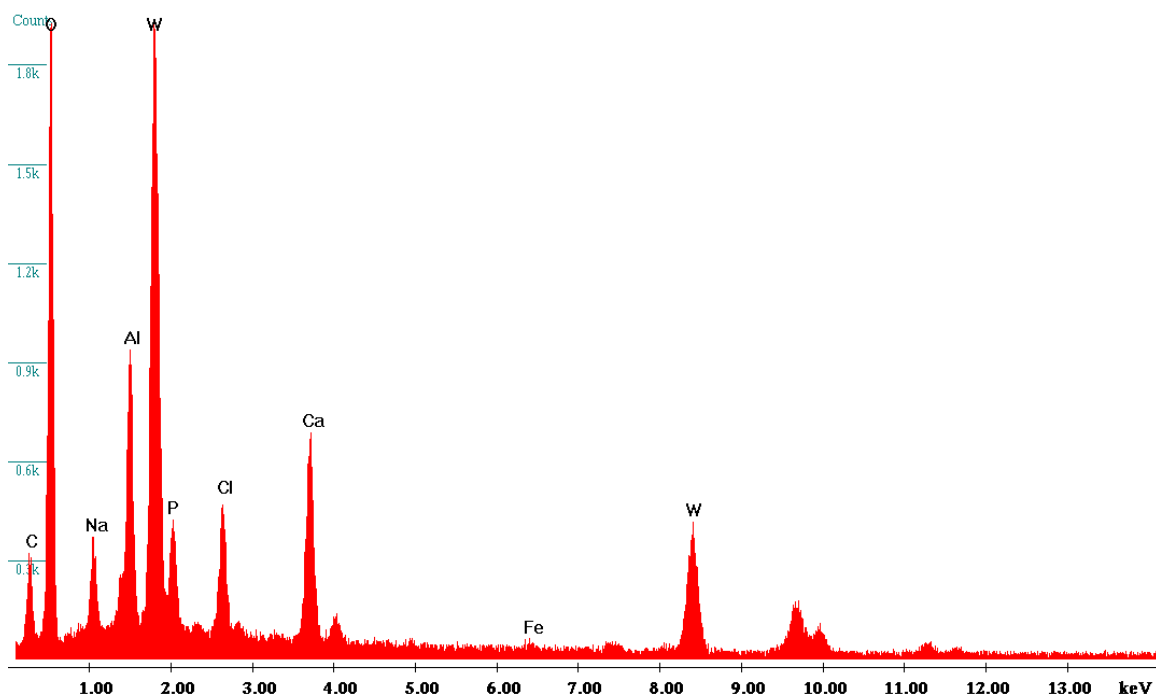
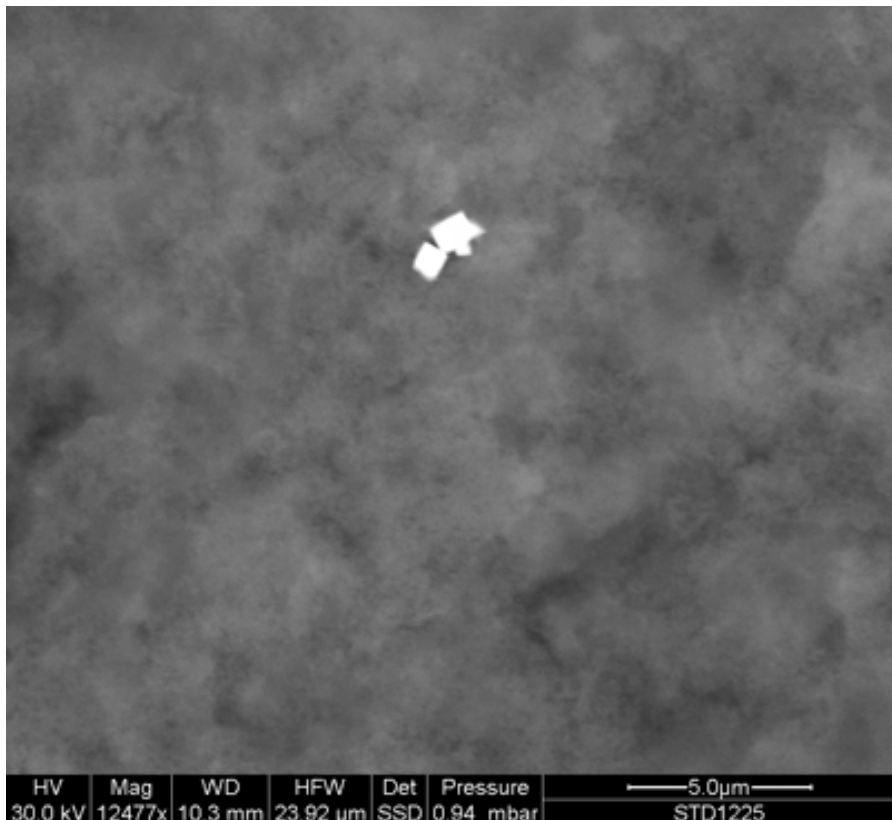


Image 27. The photograph at high magnification (2895x) shows a debris slightly larger than 1 micron whose composition is Oxygen, Tungsten, Aluminum, Calcium, Chlorine, Sodium, Phosphorous, Carbon and Iron.



HV Mag WD HFW Det Pressure
30.0 kV 12477x 10.3 mm 23.92 μm SSD 0.94 mbar

— 5.0 μm —
STD1225

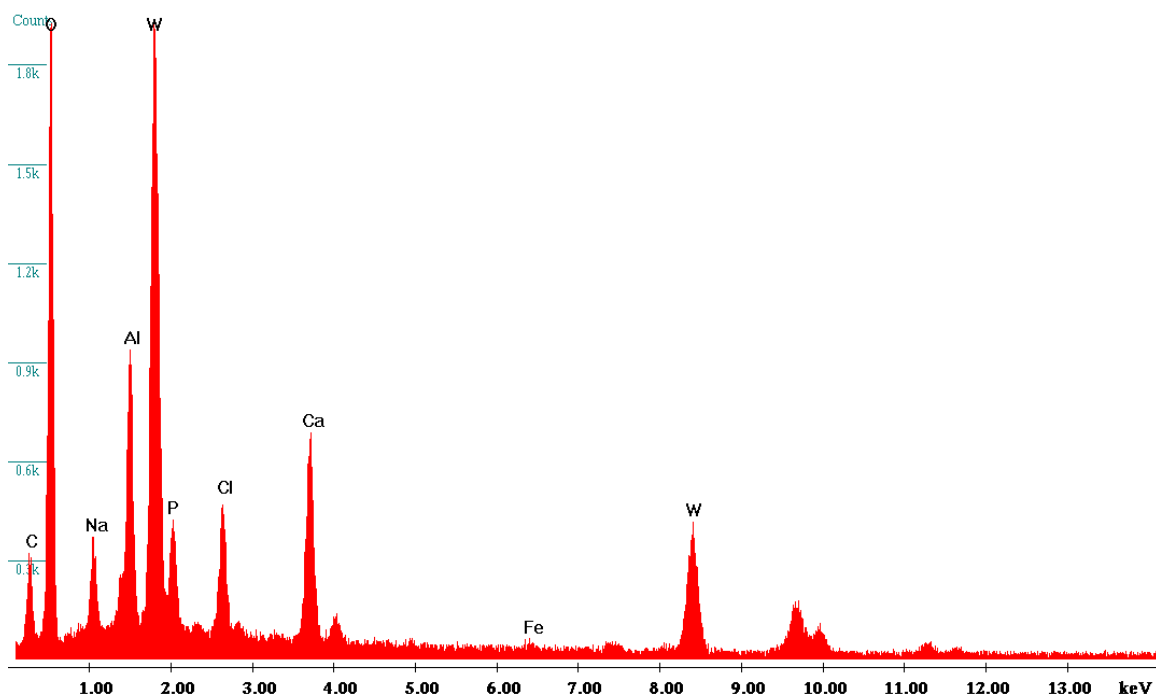
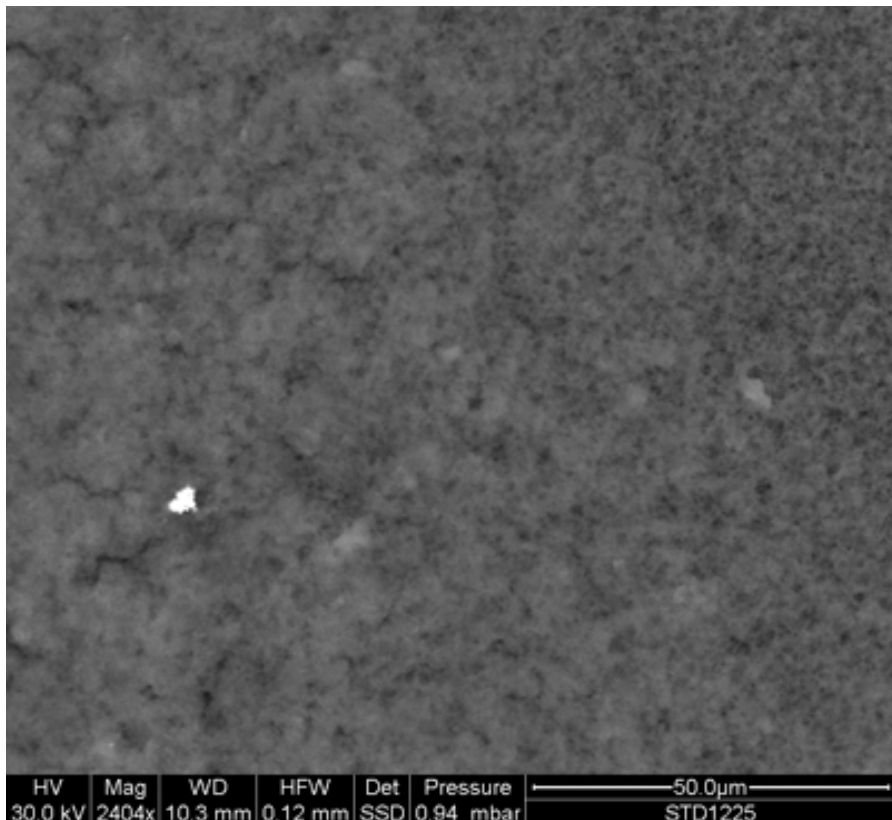


Image 28. At high magnification (12477x) three particles are shown with a squared morphology, only one of which is larger than 1 micron. Like many other particles detected in the sample, also they are made of Oxygen, Tungsten, Aluminum, Calcium, Chlorine, Sodium, Phosphorous, Carbon and Iron.



HV Mag WD HFW Det Pressure ━━━━ 50.0µm ━━━━
30.0 kV 2404x 10.3 mm 0.12 mm SSD 0.94 mbar STD1225

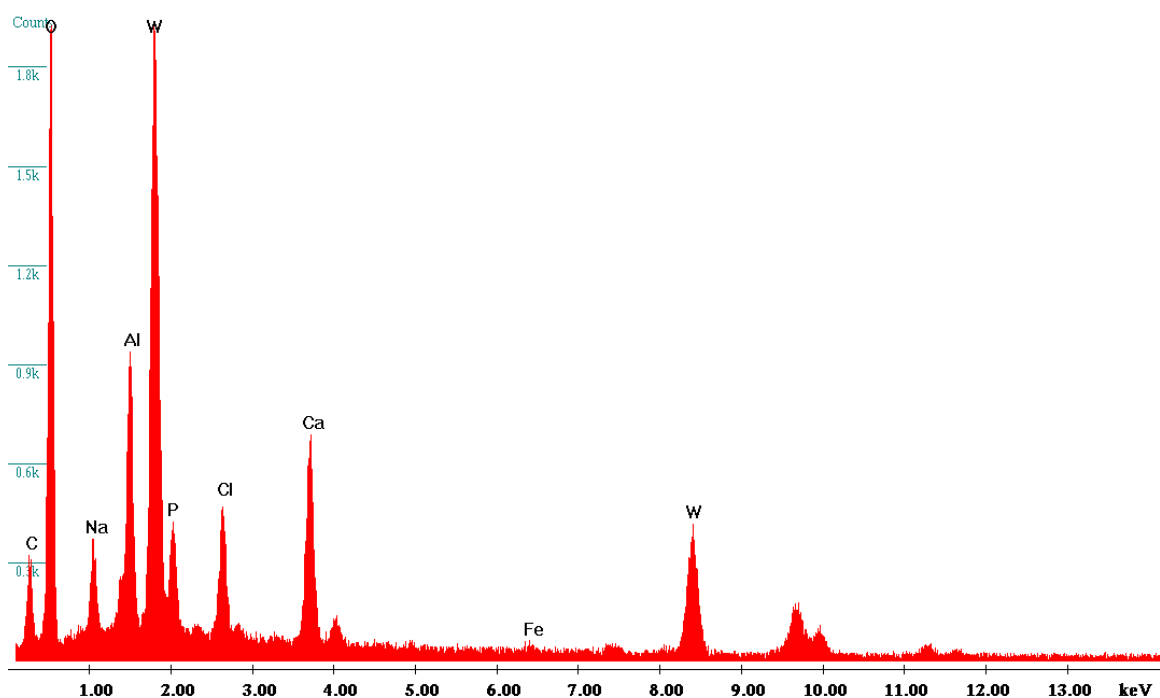


Image 29. At a magnification of 2404x a group of particles can be seen: Their composition detected at EDS, like that of many other particles found in this sample, is Oxygen, Tungsten, Aluminum, Calcium, Chlorine, Sodium, Phosphorous, Carbon and Iron.

6. DISCUSSION AND CONCLUSIONS

The sample of vaccine Infanrix checked contains a relevant number of solid, inorganic particles. We identified 3 different compositions: Stainless steel (Iron-Chromium-Nickel-Manganese-Silicon), Titanium, and mostly Tungsten. The composition obtained subtracting the background of Aluminum-Phosphorus-Sodium-Chlorine is Tungsten-Calcium-Sulfur-Iron. The particles detected are micron- and submicron- and nano-sized, and some have a square morphology. They might be the result of a technological (or nanotechnological) process. Their aggregation is typical of nanoparticles, a phenomenon due to their high surface energy. The presence of those particles is not listed among the ingredients reported in the data sheet and, in any case, it is not clear why they are there. Judging by their composition, they are not soluble either in water and in fats, are not biodegradable and are not compatible with the human organism.

As far as pathogenicity is concerned, their most important feature is their small size, often below one micron. It is a well-known fact that the smaller the particle, the more capable it is of penetrating tissues and even cell nuclei where they can interfere with the DNA (3). Besides being bodies foreign to human histology and, because of that, triggering factors of inflammatory reactions (chronic reactions, being they non biodegradable), due to their small size the ratio between external surface and volume is very high and, as a consequence, their reactivity is particularly elevated.

Apart from some particles of different composition (for example one with a very high presence of Titanium), the vast majority of them is composed of Oxygen, Tungsten, Aluminum, Calcium, Chlorine, Sodium, Phosphorous, Carbon and Iron.

While the presence of Oxygen, Aluminum, Calcium, Chlorine, Sodium, Phosphorous and Carbon could find an explanation (though certainly not in particulate form) as rightful components of the vaccine, Titanium, Stainless steel and Tungsten are a puzzle. Tungsten, in particular, has been detected with a very high frequency.

It must be emphasized that the pathogenicity of micro-, and, above all, nanoparticles is only partially dependent on dose and composition. References show the impact of nanoparticles on human body and cells (4-28). Among other factors, their capability of inducing an adverse reaction to the organism is related to their size, their

shape and the tissue or organ the blood flow had carried them to, a variable actually impossible to predict.

The World Health Organization defines particulate matter sized 2.5 micron or less as class-1 carcinogen, namely, they can induce cancer (51).

As a matter of fact, it is impossible to predict where the blood flow will carry those particles. Thus, their possible adverse effects depend on the target they hit and the dilution at which they hit it. When dilution is high enough, the effects are very often not clinically visible.

7. REFERENCES

1. A.M. Gatti, M. Ballestri, A. Bagni, Granulomatosis associated to porcelain wear debris, American Journal of Dentistry 2002, 15(6): 369-372.
2. A.M. Gatti Biocompatibility of micro- and nano-particles in the colon (part II) Biomaterials 2004, vol.25, 3, Feb 385-392. -
http://nano.cancer.gov/resource_center/sci_biblio_devices-machines.asp
3. A.M. Gatti, S. Montanari " Approccio bioingegneristico alla Sindrome dei Balcani" Fisica in Medicina 2004, n.2 , 107-114.
4. K. Peters, R. Unger, A.M. Gatti, E. Monari, J. Kirkpatrick Effects of nano-scaled particles on endothelial cell function in vitro: Studies on viability, proliferation and inflammation, J. of Material Science: Mat. in Medicine 2004, 15 (4), 321-325.,
5. A.M. Gatti, S. Montanari, E. Monari, A. Gambarelli, F. Capitani, B. Parisini Detection of micro and nanosized biocompatible particles in blood. J. of Mat. Sci. Mat in Med. 2004, 15 (4): 469-472.
6. A.M. Gatti, S. Montanari, Risk assessment of micro and nanoparticles and the human health, capitolo di H.S. Nalwa - Handbook of Nanostructured biomaterials and their applications - American Scientific Publisher USA 2005, cap. 12, 347-369.
7. S. Divertito, A. Gatti Le nanoparticelle assassine Capitolo n. 4 sul libro Uranio:il nemico invisibile, Infinito Edizioni, Roma, 2005
8. A.M. Gatti Uranio impoverito. Neoplasie e alte temperature. La morte a forma di sfera la Rinascita 2005, Marzo, p.117-24.

9. A.M. Gatti, S. Montanari, Retrieval analysis of clinical explanted vena cava filters J. of Biomedical Materials Research: Part B. 2006, 77B, 307-314, .
10. A.M. Gatti, S. Montanari, A. Gambarelli, F. Capitani, R. Salvatori In-vivo short- and long-term evaluation of the interaction material-blood Journal of Materials Science Materials in Medicine, 2005, 16, 1213-19
11. S. Montanari, A.M. Gatti Nanopathology and nanosafety. Proceedings of the international School on advance material science technology VII Course, "Nanotechnologies for drug delivery and medical applications. Iesi, settembre 2005
12. G. Barbolini, A.M. Gatti, Nanopatologia. Trattato di Istopatologia. Ed. Piccin Nuova Libraria Padova 2006, Cap.1.5 pag 75-80
13. G. Barbolini, A.M. Gatti, B. Murer, Pleura, Trattato di Istopatologia. Ed. Piccin Nuova Libraria Padova 2006, Cap 8.4 pag 1081-1098 .
14. K. Peters, R. Unger, A.M. Gatti, E. Sabbioni, A. Gambarelli, J. Kirkpatrick, Impact of ceramic and metallic nanoscaled particles on endothelial cell functions in vitro. Nanotechnologies for the life Sciences Vol.5 Nanomaterials- Toxicity, Health and Environmental Issues Ed. By Challa S.S. R. Kumar Wiley –VCH Verlag GmbH &Co. KGaA 2006. vol. 5, 108-125.
15. A.M. Gatti, L'inquinamento bellico come causa di nanopatologie capitolo del libro "URANIO", M.I.R. Edizioni, novembre 2005 pag. 6-35,
16. T. Hansen, G. Clermont, A. Alves, R. Eloy, C. Brochhausen, J.P. Boutrand, A.M. Gatti, J. Kirkpatrick, Biological tolerance of different materials in bulk and nanoparticulate form in a rat model: Sarcoma development by nanoparticles J. R. Soc. Interface (2006) 3, 767-775
17. S. Montanari, A.M. Gatti Nanopatologie: Cause ambientali e possibilità di indagine. Ambiente Risorse Salute n. 110 Settembre ottobre 2006, 18-24.
18. A.M. Gatti, M. Ballestri, G. Cappelli Nanoparticles: potential toxins for the organism and the kidney? CRITICAL CARE NEPHROLOGY, 2nd Edition, Basic Physiology, 2007 Chapter 235 :
19. S. Montanari Nanopatologie, ambiente e inceneritori – Medicina Democratica 168/172 (2007) pagg. 51-58
20. S. Montanari Il girone delle polveri sottili Ed. Macro 2008
21. A.M. Gatti, S. Montanari "Nanopathology" Ed. Pan Stanford 2008, 1-212.

22. S. Montanari "L'insidia delle poveri sottili e delle nanoparticelle", Ed. Macro 2007,
23. A.M. Gatti, S. Montanari Nanopollution: The Invisible Fog of Future Wars – The Futurist (May-June 2008) pagg. 32-34
24. Montanari S., Gatti A.M. – Inquinamento involontario da micro e nanoparticolato inorganico negli alimenti – La Rivista di Scienza dell'Alimentazione, numero 2, aprile-giugno 2008, anno 37, pagg. 17-28
25. A.M. Gatti, D. Tossini, A. Gambarelli, S. Montanari, F. Capitani – Investigation of the Presence of Inorganic Micron- and Nanosized Contaminants in Bread and Biscuits by Environmental Scanning Electron Microscopy – Critical Reviews in Food Science and Nutrition, 49:275-282 (2009)
26. Antonietta M. Gatti, Daniela Quaglino, Gian Luca Sighinolfi, A Morphological Approach to Monitor the Nanoparticle-Cell Interaction International Journal of Imaging (ISSN 0974-0627) Volume 2 No. S09 Spring 2009 (Editorial 1) 2-21
27. A.M. Gatti, S. Montanari – Nanocontamination of the soldiers in a battle space – capitolo di I. Linkov e J. Steevens (eds.) – Nanomaterials: Risks and Benefits – Springer Science + Business Media B.V. 2009 – pagg. 83 – 92
28. Rapporto del presidente della Commissione Uranio Impoverito- XV legislatura (<http://www.senato.it/commissioni/41378/95052/genpagina.htm>)
29. A.M. Gatti, S. Montanari – Nanopathology: A Controversial Aspect of Nanomedicine – Nanomagazine – Nov. 2011 (17-21)
30. Antonietta M. Gatti, Paolo Bosco, Francesco Rivasi, Sebastiano Bianca, Giuseppe Ettore, Luigi Gaetti, Stefano Montanari, Giovanni Bartoloni, Diego Gazzolo, Heavy metals nanoparticles in fetal kidney and liver tissues, Frontiers in Bioscience (Elite edition, E3) 2011;1 (January):221-6
31. A.M. Gatti, S. Montanari – Nanoparticles: A New Form of Terrorism? – capitolo 4 in A. Vaseashta et al. (eds.) Technological Innovations in Sensing and Detection of Chemical, Biological, Radiological, Nuclear Threats and Ecological Terrorism, NATO Science for Peace and Security Series A: Chemistry and Biology (pagg.45-53)
32. Nemmar A., Hoet P.H.M., Vanquickenborne B., Dinsdale D., Thomeer M., Hoylaerts M..F., Vanbilloen H., Mortelmans L., Nemery B. (2002). Passage of inhaled particles in to the blood circulation in humans, Circulation, 105 (4), pp.411-417.

33. Oberdörster G, Sharp Z, Atudorei V, Elder A, Gelein R, Kreyling W, Cox C., Translocation of inhaled ultrafine particles to the brain. *Inhal Toxicol.* 2004 Jun;16(6-7):437-45.
34. Elder A, Oberdörster G. Translocation and effects of ultrafine particles outside of the lung. *Clin Occup Environ Med.* 2006;5(4):785-96. Review.
35. Elder A, Gelein R, Silva V, Feikert T, Opanashuk L, Carter J, Potter R, Maynard A, Ito Y, Finkelstein J, Oberdörster G. Translocation of inhaled ultrafine manganese oxide particles to the central nervous system. *Environ Health Perspect.* 2006 Aug;114(8):1172-8. Erratum in: *Environ Health Perspect.* 2006 Aug;114(8):1178.
36. Annette Peters, Bellina Veronesi, Lilian Calderón-Garcidueñas, Peter Gehr, Lung Chi Chen, Marianne Geiser, William Reed, Barbara Rothen-Rutishauser, Samuel Schürch, and Holger Schulz, Translocation and potential neurological effects of fine and ultrafine particles a critical update. Part Fibre Toxicol. 2006; 3: 13.
37. Kenneth W. Rundell, Jay R. Hoffman, Renee Caviston, Ronald Bulbulian, and Amanda M. Hollenbach, Inhalation of Ultrafine and Fine Particulate Matter Disrupts Systemic Vascular Function, *Inhalation Toxicology*, 19:133–140, 2007
38. PE Schwarze, J Øvrevik, M La^øg, M Refsnes, P Nafstad, RB Hetland and E Dybing, Particulate matter properties and health effects: consistency of epidemiological and toxicological studies *Human & Experimental Toxicology* (2006) 25: 559 -579
39. Andre Nel,^{1,2*} Tian Xia,¹ Lutz Ma^ødler,³ Ning Li¹ Toxic Potential of Materials at the Nanolevel *SCIENCE VOL 311 3 FEBRUARY 2006* 627.
40. Tran CL, Buchanan D, Cullen RT, Searl A, Jones AD, Donaldson K: Inhalation of poorly soluble particles. II. Influence Of particle surface area on inflammation and clearance. *Inhal Toxicol* 2000, 12:1113-1126.
41. Schwartz J: What are people dying of on high air-pollution days. *Environmental Research* 1994, 64:26-35.
42. Nemmar A, Hoylaerts MF, Hoet PH, Vermeylen J. 2003, Size effect of intratracheally instilled particles on pulmonary inflammation and vascular thrombosis. *Toxic. Appl. Pharmacol.* 186, 38-45.
43. Moeller W, Felten K, Sommerer K, Scheuch G, Meyer G, Meyer P, Haussinger K, Kreyling WG. Deposition, Retention and Translocation of Ultrafine Particles from the

Airways and Lung Periphery. Am J Respir Crit Care Med. 2007 Oct 11; [Epub ahead of print]

44. Borm PJ, Robbins D, Haubold S, Kuhlbusch T, Fissan H, Donaldson K, Schins R, Stone V, Kreyling W, Lademann J, Krutmann J, Warheit D, Oberdorster E. The potential risks of nanomaterials: a review carried out for ECETOC. Part Fibre Toxicol. 2006 Aug 14;3:11.
45. Frampton MW, Stewart JC, Oberdörster G, Morrow PE, Chalupa D, Pietropaoli AP, Frasier LM, Speers DM, Cox C, Huang LS, Utell MJ. Inhalation of ultrafine particles alters blood leukocyte expression of adhesion molecules in humans. Environ Health Perspect. 2006 Jan;114(1):51-8.
46. Yuliang Zhao, Hari Singh Nalwa, Nanotoxicology - Interactions of Nanomaterials with Biological Systems, (2006);
47. A. Elder, I. Lynch, K. Grieger, S. Chan-Remillard, A.M. Gatti, H. Gnewuch, E. Kenawy, R. Korenstein, T. Kuhlbusch, F. Linker, S. Matias, N. Monteiro-Riviere, V.R.S. Pinto, R. Rudnitsky, K. Savolainen, A. Shvedova – Human Health Risks of Engineered Nanomaterials: Critical Knowledge Gaps in Nanomaterials Risk Assessment - capitolo di I. Linkov e J. Steevens (eds.) – Nanomaterials: Risks and Benefits – Springer Science Business Media B.V. 2009 – pagg. 3 – 30
48. Urban RM, Jacobs JJ, Gilbert JL, Galante JO, Migration of corrosion products from modular hip prostheses. Particle microanalysis and histopathological findings, The Journal of Bone and Joint Surgery. American Volume [1994, 76(9):1345-1359]
49. Kirkpatrick CJ, Barth S, Gerdes T, Krump-Konvalinkova V, Peters K., Pathomechanisms of impaired wound healing by metallic corrosion products. Mund Kiefer Gesichtschir. 2002 May;6(3):183-90.-
50. Lee SH, Brennan FR, Jacobs JJ, Urban RM, Ragasa DR, Glant TT, Human monocyte/macrophage response to cobalt-chromium corrosion products and titanium particles in patients with total joint replacements. J Orthop Res. 1997 Jan;15(1):40-9.
51. International Agency for Research on Cancer – World Health Organization – Press release n. 221/17-10-2013